

**DEVELOPMENT OF SOFTCOPY
PHOTOGRAMMETRIC
AND
CHROMO-STEREOSCOPIC SYSTEM**

*A Thesis Submitted
in Partial Fulfilment of the Requirements
for the Degree of*

MASTER OF TECHNOLOGY

by

EDULA PANDU RANGA REDDY

to the

**DEPARTMENT OF CIVIL ENGINEERING
INDIAN INSTITUTE OF TECHNOLOGY
KANPUR**

June, 1997

-6 AUG 1997
CENTRAL LIBRARY
L.I.T., KANPUR

Vol. No. A 123654

CERTIFICATE

Certified that the work presented in this thesis entitled
**“Development of Softcopy Photogrammetric and
Chromo-stereoscopic System”** by **Mr. Edula Pandu
Ranga Reddy** has been carried out under my
supervision and has not been submitted elsewhere for
any degree.

16th June, 1997

Nitin Kumar Tripathi
16.6.97

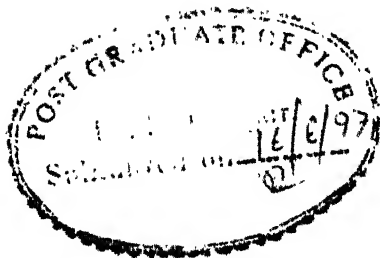
(Nitin Kumar Tripathi)

Assistant Professor

Department of Civil Engineering

Indian Institute of Technology

Kanpur



ABSTRACT

The present study is oriented to investigate the appropriate approach for satellite digital photogrammetry. SPOT-PLA stereoscopic data of an area near Pune has been used. Non-parametric approach with first order polynomial equations has been utilised for epipolar geometry. Chromo-stereoscopic concept has been implemented to generate chromo-stereoscopic picture of the study area, which produces 3D view of the region when seen by chroma-depthTM glasses.

An user friendly - interactive software in C-language and STARBASE graphics on UNIX platform has been generated. This has modules such as generation of height map, height classified map, surface representation in mesh and solid models, slope classified maps, and contours. The software presents robust capability of data input, data analysis, conversion, height determination and data output in various forms.

The study presents an alternative, not only to analogue photogrammetry but also to expensive and unaffordable hardware and software sold by vendors across the world. The present software has been developed in general way so that it can be ported to other platforms with few modifications. The output of this study in form of DTM, contour map, slope map, chromo-stereoscopic visualisation etc., may be used for developmental and hazard mitigation projects.

Acknowledgements

I express my sincere gratitude to Dr. Nitin Tripathi for his consistent help and valuable guidance throughout my thesis work.

I thank Dr. Onkar Dikshit and Dr. B. C. Raymahashay for their constant motivation, expert guidance and advice at various stages of thesis work.

I thank Mr. K. Venu Gopal Rao, scientist, NRSA, for his consistent advice and help.

My heartiest gratitude to the faculty members of Civil Engineering who imparted sound and in-depth knowledge during my course work.

I also thank Mr. G. P. Mishra, Mr. Ram Kishan and Mr. Shukla for the help rendered by them.

Special thanks to Ram Prasad, Siva, U rao, S. Giri, Srikanth, Eswar, Shanthi Kumar, Polavara, Giridhar, Dip, Suresh, Ashraf, T. K. Das, B. K. Rai and other friends for their unreserved help.

Thanks are due to my friends in Hall-V and Hall-IV for their motivation and for making my stay at IIT Kanpur memorable.

I take great pride in acknowledging my parents and family members for their constant encouragement and inspiration.

TO
MY PARENTS
AND
SISTERS

CONTENTS

PAGE

LIST OF TABLES	iv
LIST OF FIGURES	v
ABSTRACT	
CHAPTER 1	INTRODUCTION
	1.0 General 1-1
	1.1 Softcopy Photogrammetry System 1-2
	1.2 Advantages of Softcopy Photogrammetric System 1-3
	1.3 Deneration of Digital Terrain Model in 20th Century 1-4
	1.4 Scope and Objective of Work 1-5
	1.5 Study Area and Data used 1-5
	1.6 Organisation of the Work 1-6
CHAPTER 2	LITERATURE REVIEW
	2.0 Softcopy Photogrammetry 2-1
	2.1 Digital Terrain Model (DTM) 2-2
	2.1.1 Data Acquisition 2-2
	2.1.1.1 Ground survey method 2-4
	2.1.1.2 Graphic digitizing methods 2-4
	2.1.1.3 Photogrammetric methods 2-5
	2.1.2 Stereo plotting instruments 2-5
	2.1.2.1 Optical projection instruments 2-6
	2.1.2.2 Mechanical projection system 2-6
	2.1.2.3 Analytical photogrammetric instrumentation 2-7
	2.1.3 Stereo matching methods 2-11

2.1.3.1	Area-based matching	2-11
2.1.3.1.1	Matching based on correlationcoefficient	2-11
2.1.3.1.2	Matching based on least squares	2-14
2.1.3.2	Feature-based matching	2-15
2.1.3.3	Hybried model	2-17
2.2	Satellites with Stereo Data Capability	2-17
2.2.1	SPOT	2-17
2.2.1.1	SPOT mission specifications	2-18
2.2.1.2	Stereoscopic ability of SPOT	2-20
2.2.2	IRS-1C	2-20
2.3	Earlier Works on DTM Generation	2-21
2.4	Chromo-Stereoscopy	2-24
CHAPTER THREE	METHODOLOGY AND RESULTS	
3.1	Digital stereo pair acquisition from satellite	3-1
3.2	Establishing Epipolar Geometry	3-1
3.2.1	Geometric rectification	3-3
3.2.1.1	Spatial interpolation	3-4
3.2.1.2	Intensity Interpolation	3-6
3.3	Parallax Determination	3-9
3.3.1	Area-based matching	3-9
3.4	DTM computation	3-10
3.5	Generation of Height Map	3-10
3.6	Generation of Height Classified Map	3-11
3.7	Generation of Solid Model	3-11
3.8	Generation of Mesh Model	3-11
3.9	Generation of Slope Map	3-12
	RESULTS	3-13
CHAPTER FOUR	CHROMO-STEREOSCOPY	
4.1	Introduction	4-1
4.1.1	Eye: biological phenomena	4-2
4.1.2	Colour	4-2

	4.1.3 Visual Depth Perception	4-3
	4.2 Stereo Contemplation Approaches	4-4
	4.3 Chromo-Stereoscopy	4-5
	4.4 Methodology	4-7
	4.5 Analysis of Chromo-Stereoscopes	4-9
	4.6 Conclusion	4-11
CHAPTER FIVE	SOFTWARE DEVELOPMENT	
	5.1 Hardware and Compilers	5-1
	5.2 Geometric Correction	5-1
	5.2.1 GCP generation	5-1
	5.2.2 Registration	5-1
	5.3 Cross-Correlation and Height Determination	5-2
	5.4 Input File for Display of Display	5-2
	5.5 Core System	5-2
	5.5.1 Display of Image	5-2
	5.5.2 Display of Height Map	5-2
	5.5.3 Height Classified Map	5-3
	5.5.4 Mesh Model of Relief Data	5-3
	5.5.5 Solid Model of Surface	5-3
	5.5.6 Chromo-Stereoscopic module	5-4
	5.5.7 Slope Map	5-4
	5.5.8 Contours	5-4
	5.5.9 Output	5-5
	5.5.10 List	5-5
	5.5.11 Exit	5-5
CHAPTER SIX	CONCLUSIONS AND FUTURE RECOMMENDATIONS	
	6.1 Conclusions	6-1
	6.2 Future Recommendations	6-2
REFERENCES		

LIST OF TABLES

Number	Title	Page
2.1	Accuracy Analysis by Cappellini <i>et al.</i>	2-23
2.2	DNM DTM accuracy results	2-23
2.3	Red Deer DTM accuracy results	2-23
3.1	GCPs Position in Left and Right Stereo Imagery	3-16
3.2	Evaluation error summary at few selected points	3-17
3.3	Frequency distribution errors at selected points	3-17

LIST OF FIGURES

Number	Title	Page
1.1.a	Study Area: South West of Pune	1-7
1.1.b	Test Site Co-ordinates	1-8
1.2	SPOT Stereo-pair	1-9
2.1	Epipolar Geometry	2-3
2.2	Optical stereo projection	2-8
2.3	Mechanical stereo projection instrument	2-8
2.4	Flow chart of comparator and off line solution	2-10
2.5	Flow chart of comparator and on line solution	2-10
2.6	Area-based parallax matching principle	2-13
2.7	Flow chart for feature-based stereo matching	2-16
2.8	Stereoscopic scanning process of SPOT	2-19
3.1	Flow chart for computation of DTM	3-2
3.2	Pictorial computation of:	
3.2.a	Nearest Neighbourhood method	3-7
3.2.b	Bilinear Interpolation	3-7
3.2.c	Cubic convolution method	3-7
3.3	Correlation coefficient analysis on 3×3 target window	3-18
3.4	Correlation coefficient analysis on 5×5 target window	3-18
3.5	Correlation coefficient analysis on 7×7 target window	3-19
3.6	Correlation coefficient analysis on 9×9 target window	3-19
3.7	Correlation coefficient analysis on 11×11 target window	3-20
3.8	Correlation coefficient analysis on 13×13 target window	3-20
3.9	Unitary time results for different target window sizes	3-21
3.10	Height Intensity Map	3-22
3.11	Height Classified Map	3-22
3.12.a	Mesh Model of Top Left Region	3-23
3.12.b	Mesh Model of Top Right Region	3-23

3.12.c	Mesh Model of Bottom Left Region	3-24
3.12.d	Mesh Model of Bottom Right Region	3-24
3.13.a	Solid Model of Top Left Region	3-25
3.13.b	Solid Model of Top Right Region	3-25
3.13.c	Solid Model of Bottom Right Region	3-26
3.13.d	Solid Model of Bottom Right Region	3-26
3.14	Slope Classified Map	3-27
3.15	Contour with Surface Representation	3-27
3.16	Block diagram of contour plots of test area	3-28
4.1	Variation of refraction index with respect to material and wavelength	4-6
4.2.a	Single prism glass configuration	4-6
4.2.b	Double prism glass configuration	4-6
4.3	Flow chart for generating Chromo-Stereoscopic image	4-8
4.4	Chromo-Stereoscopic Image	4-10
5.1	Softcopy Photogrammetric and Chromo-Stereoscopic System	5-6

CHAPTER ONE

INTRODUCTION

1.0 General

Civil engineering projects world wide have many diverse and important encounters with elevation of terrain. All civil engineering structures such as road networks, hydraulic networks, bridges, reservoirs are directly or indirectly dependent on height of the terrain. The knowledge of height, influences the design and placement of structures.

Terrain information is generally obtained by surveying methods. But this is very costly and time consuming when carried on large scale. Search for an alternative method and sources for generating terrain information for large areas are carried and the science of photogrammetry was invented. In this, a single area is photographed from two different positions. Any apparent change in position of an object present on the image is due to the relief of the object. This apparent shift in the position of the object in stereo images is called parallax. By measuring this parallax the height information of the object can be determined.

In India, information about terrain is generally available with the Survey of India, in form of toposheets. Toposheets are available at variable scales ranging from 1: 25000 to 1: 100000, with the contour interval ranging from 20 to 100m. This information is very useful in various fields of civil engineering. Toposheets are generally revised at an interval of 10 - 20 years with respect to their demand and importance. The present day requirement is the current terrain map and elevation data of the area at frequent interval and low cost. To provide the height information at comparatively low cost, satellites with stereo scanning facilities were launched. First among this is SPOT, a French satellite (with

a spatial resolution of 10m) and recently followed by IRS-1C (spatial resolution of 5.8m). Image data is supplied in form of reflectance digital record. The terrain elevation is determined by using photogrammetric principles, but the difference lies in the way of application of the principles. This resulted in the birth of a completely new field called Digital Photogrammetry, commonly known as Softcopy Photogrammetry.

Attempts to process aerial or satellite image data automatically was first reported by Rosenberg in the early 1950s (Rosenberg, 1955). With the advent of digital image processing technology, a new level of flexibility in algorithmic design emerged. Digital processing of space images, medical and other "non-conventional" imagery were among the earliest applications. This technology however, because of its new field of learning, was not available for the great majority of the photogrammetric community. Only recently have the advancements in semiconductor technology, micro-electronics and the related decline of costs caused severe change in the availability of digital stereo technology and digital processing systems. Contemporary photogrammetry has inculcated changes in working tools and is reaching out for the latest technology and the opportunity to enter new applications. From the discovery of photography, it took about one century to the first analogue instruments, and from there it took another half a century to the introduction of analytical plotters into the civilian practice. But it took only 12 years to introduce the new class of processing instruments: the Digital Photogrammetric System.

1.1 Softcopy Photogrammetry System

A Softcopy Photogrammetric System is one which consists of software and hardware to carry out photogrammetric tasks in an interactive and automated way using digital image as input (Gruen, 1989).

Analogue and analytical photographic data processing is characterised by a great variety of different instruments e.g., comparators, stereo plotters, rectifiers, orthoprojectors. These vary greatly with respect to design, construction, universality, flexibility, accuracy, usage,

control, input, and output. Only the analytical plotters feature a certain degree of task integration i.e., they allow execution of different types of tasks on the same instrument.

In Softcopy Photogrammetric System total image may not have to be processed, only small packets of image may be used for display. Once the interior orientation of the image is established the geometric definition of the image is recorded. This relieves the operator from the re-establishing the interior orientation in the case of remeasurement of the previously used imagery. The resampling results in a much better refined imagery, which results in better accuracy of the derived products. This reduction to the strict perspective model leads to a great simplification of the formulae which are used for processing.

In general, Softcopy Photogrammetric Systems allows execution of otherwise expensive and time consuming procedures both rapidly and efficiently, with the prospect of attaining new levels of accuracy in the case of automatic processing.

1.2 Advantages of Softcopy Photogrammetry System

A Softcopy Photogrammetric System is distinguished by a number of points from conventional photogrammetric instruments (Gruen, 1989).

1. No high precision optical - mechanical parts required.
2. Robust measurement system; no wear and tear.
3. No instrument calibration, no manual image handling.
4. Stable images, no deformation overtime.
5. Combination of automatic and operator controlled processing.
6. High degree of interactivity.
7. Data acquisition, processing, editing, storage, and administration in a single system
8. On-line and real-time capabilities.

1.3 Generation of Digital Terrain Model in 20th Century

With the rapid advancement in technology many improvements have been incorporated at every stage in the generation of the Digital Terrain Model. But after the inductance of digital technology a complete phase change occurred in all parts of the photogrammetric applications and so also in the generation of the terrain modelling.

The data cost has reduced drastically after the launch of the satellites, but at the cost of quality of data. The spatial resolution of early satellite imageries may be less but the cost effectiveness is very high and in some projects where this resolution of data is permissible it made an revolutionary change. Now with the launch of SPOT satellite and especially IRS-1C, the latest of the Indian Remote Sensing Satellite series, satellite imageries are poised to replace conventional aerial photographs.

The construction of a 3-D model of a scene starts from a digital stereo pair, which involves the resolution of three main problems (Cappellini *et al.*, 1991):

- (i) orientation of the stereo pair into epipolar geometry
- (ii) matching of corresponding points in both the images
- (iii) determination of the 3-D co-ordinates of each point.

The first step, referred to as the epipolar alignment, can be accomplished by either parametric or non-parametric approach. The parametric approach requires all imaging parameters. A non-parametric method does not require the ancillary data that was recorded during image acquisition. This approach uses a mathematical function to bring the stereo imageries into epipolar geometry.

The second step is accomplished by means of a suitable correlation function, which gives an estimate of the match quality and confidence. In this there are two approaches: one is “area-based matching” and the other is a “feature-based matching”. In area-based

matching the correspondence of different points is determined by evaluating the similarity of areas around each pixel, in feature-based matching, the structural data are first extracted from each image separately and then a matching function is applied to find the corresponding positions.

Finally, the 3-D construction is much easier to achieve than the preceding steps once these have been accomplished, but its results are very sensitive to the accuracy of first two steps. Once a relative DTM is generated, the absolute DTM are scaled by linear least-squares techniques from ground control points of known heights.

1.4 Scope and Objective of Work

The scope of the present work is to test the performance of the non-parametric method in establishment of the images into epipolar geometry for generating the height information from the satellite stereoscopic images. To determine the best suitable target window size, with respect to the percentage of success of parallax determination process for different threshold values of the correlation coefficient.

The objective of the work is to develop a softcopy photogrammetric and chromo-stereoscopic system

1.5 Study Area and Data used

To meet the objective of this work, a good hilly terrain area is selected. The test area has its scene centre at $18^{\circ} 19' 19''$ N latitude and $73^{\circ} 36' 36''$ E longitude. This site is situated in the western ghats, and located south west to the Pune city. This area is covered in 47F/11 toposheet of Survey of India. The study area is shown in Figure 1.1.a. The corner latitude and longitude co-ordinates of test area are shown in Figure 1.1.b. Test area consists of Tanaji Sagar reservoir, with a maximum flood level of 636 meters approximately and with a few colonies of residential areas distributed over the entire

region. The right lower part of the test area is relatively flat, a non-perennial stream, Kanand, flows through that area. The test site have several eucalyptus plantations in some areas. The test area mainly consist of netted hills with their heights ranging up to 1150 meters. The names of few villages are Velhe Budruk, Kurah, Khurd, Ambi, Kadalpur.

SPOT satellite data is used in present thesis. The image consists of 1024 rows and 1024 columns. The spatial resolution of the data is 10 meters, and the radiometric resolution is 7 bits (0-127). The stereo pair is shown in Figure 1.2 and Figure 1.3. The left image is having an viewing angle of 18.0004° and -2.4004° in the right image.

1.6 Organisation of the Work

The present work is divided into six Chapters. First Chapter deals with a brief introduction of the problem and the various aspects associated with it. It also includes objective of the work and the way it is organised in subsequent chapters. Chapter two includes literature review. It gives a brief introduction to digital photogrammetry, analogue photogrammetric methods, and work done in the past related to generation of Digital Terrain Model from various satellites data and different methods are discussed. Chapter three deals with the methodology and the results, in this area based and feature based methods are discussed. It also involves the calculation of relative and absolute DTM. Chapter four is related to generation of chromo-stereoscopic image. This being very new, full details in generation of chromo-stereoscopic image are discussed. Chapter five provides information about the various height application modules present in the system, how they are developed and how to use them. Finally, Chapter six concludes the present work and briefs the future recommendations.

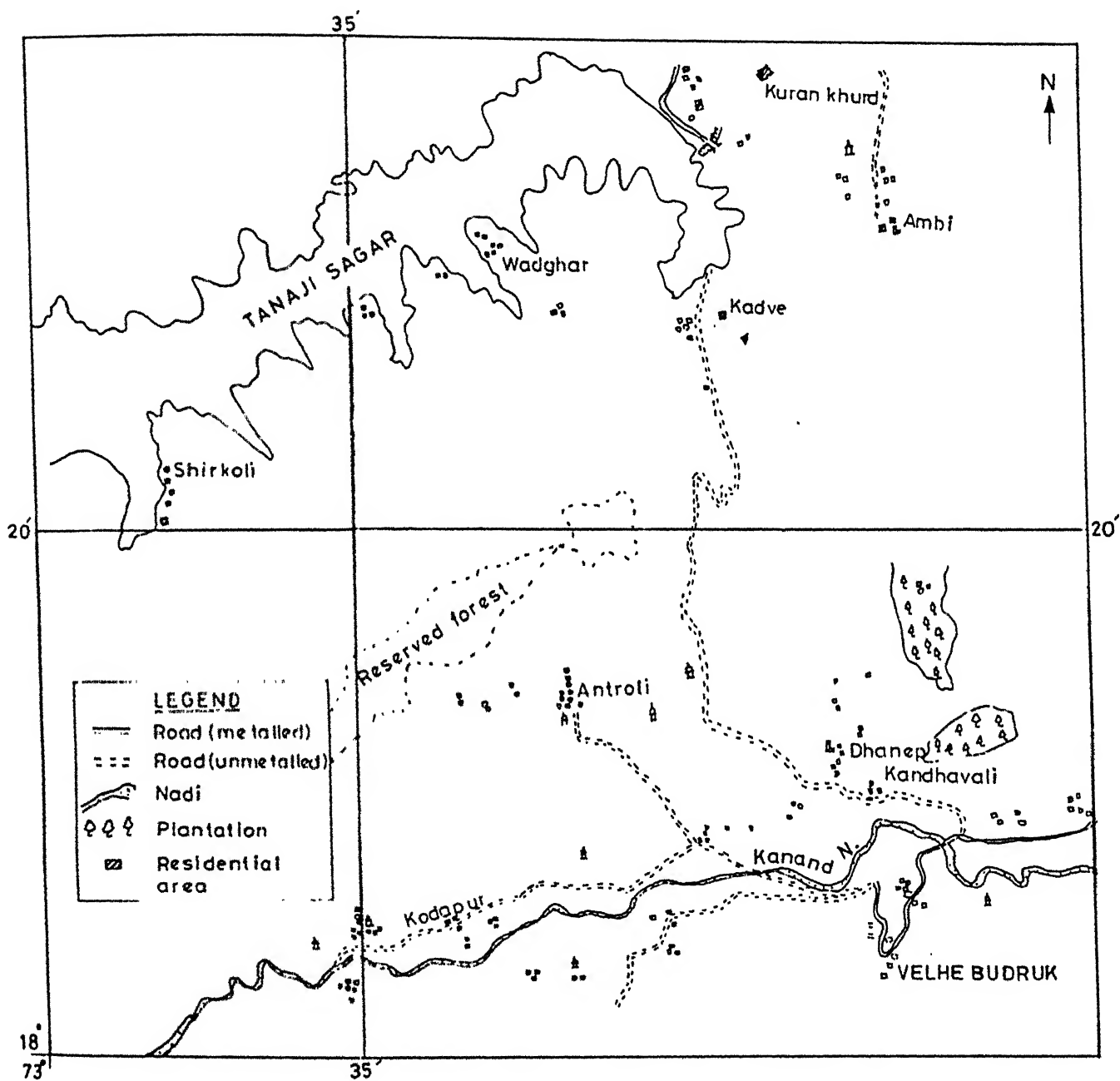


Figure 1.1a Study Area South West of Pune
(source: SOI Toposheet No. 47F/11, 1988)

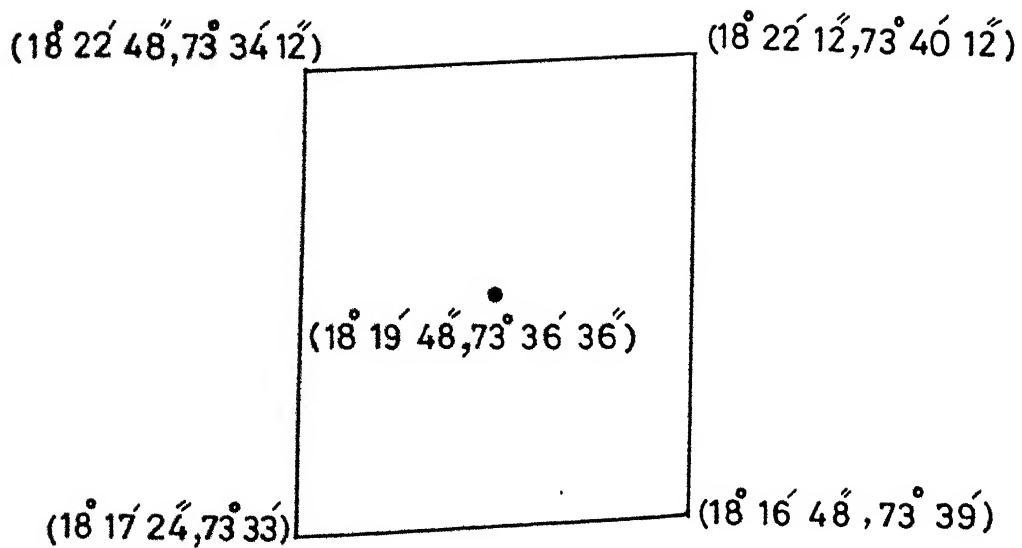


Figure 1.1.b Test site co-ordinates



Figure 1.2 Left Image of Stereo Pair



Figure 1.3 Right Image of Stereo Pair

Figure 1.2 SPOT Stereo-pair

LITERATURE REVIEW

2.0 Softcopy Photogrammetry

Softcopy Photogrammetry System is defined as one which consists of software to perform the photogrammetric tasks in an interactive and automated way using analogue photogrammetric principles on digital images.

The Softcopy Photogrammetric System have the ability to store, process, administer, output data and to perform all photogrammetric and related tasks in one system. Large number of tie points are computed by stereo matching methods, using these points, the orientation parameters along the flight trajectory and the co-ordinates of a digital elevation model are computed without external information or measurements. By analytical photogrammetric methods, the data of orientation and the DTM are computed from the image data alone.

The standard photogrammetric practice starts from the acquisition of the data.. Image of the terrain is obtained in the form of analogue form. Once the photographs are obtained, next step to be performed is the orientation of the photographs to their acquisition geometry. This process is performed by bundle adjustment.

In Digital Photogrammetry, orientation of images can be performed through any of the following two methods (Cappellini *et al.*, 1991):

1. parametric method
2. non-parametric method.

In parametric method, knowledge of the camera parameters such as focal length, absolute position and direction of view axis are required. In non-parametric method, images are oriented by using polynomial equations, by establishing the relation between ground

control points on image, and their corresponding position on the common co-ordinate system. In this method the positions of a few well distributed, well recognised points present in both the images are used. Two images are registered on to common co-ordinate system which brings the two images on to a single vertical plane. This process is known as establishment of epipolar geometry (shown in Figure 2.1). Polynomial equations are used to establish the epipolar geometry. The number of points required for first order polynomial are 3, for second order polynomial equation are 6, and for the third order polynomial equation are 10. Once the images are established in an epipolar geometry, height values are extracted by measuring the parallax. Parallax is the apparent shift in the position of the object due to change in the view position. Parallax is positive if the relief is above ground level and negative if the relief is below ground level. Parallax is determined by using stereo matching methods. The two main methods, used in evaluation of parallax, are area-based matching and feature-based matching. These two methods are discussed in detail in later part of this Chapter. The parallax is used to calculate the relative and absolute digital terrain models.

2.1 Digital Terrain Model (DTM)

Digital Terrain model is a form of computer surface modelling representing the surface of Earth numerically (Kennie and Petrie, 1990). The input to digital terrain model is the terrain elevation data, this data can be either calculated directly from this field using field surveying methods or from the indirect source like stereo-photographs or images or by digitizing the contours from topographic maps.

2.1.1 Data Acquisition

Data acquisition is very important in terrain modelling. There are three main methods which can be used to acquire elevation data. They are:

1. Ground survey methods normally using very advanced and precise equipment like electronic tacheometer or total stations with data collectors.

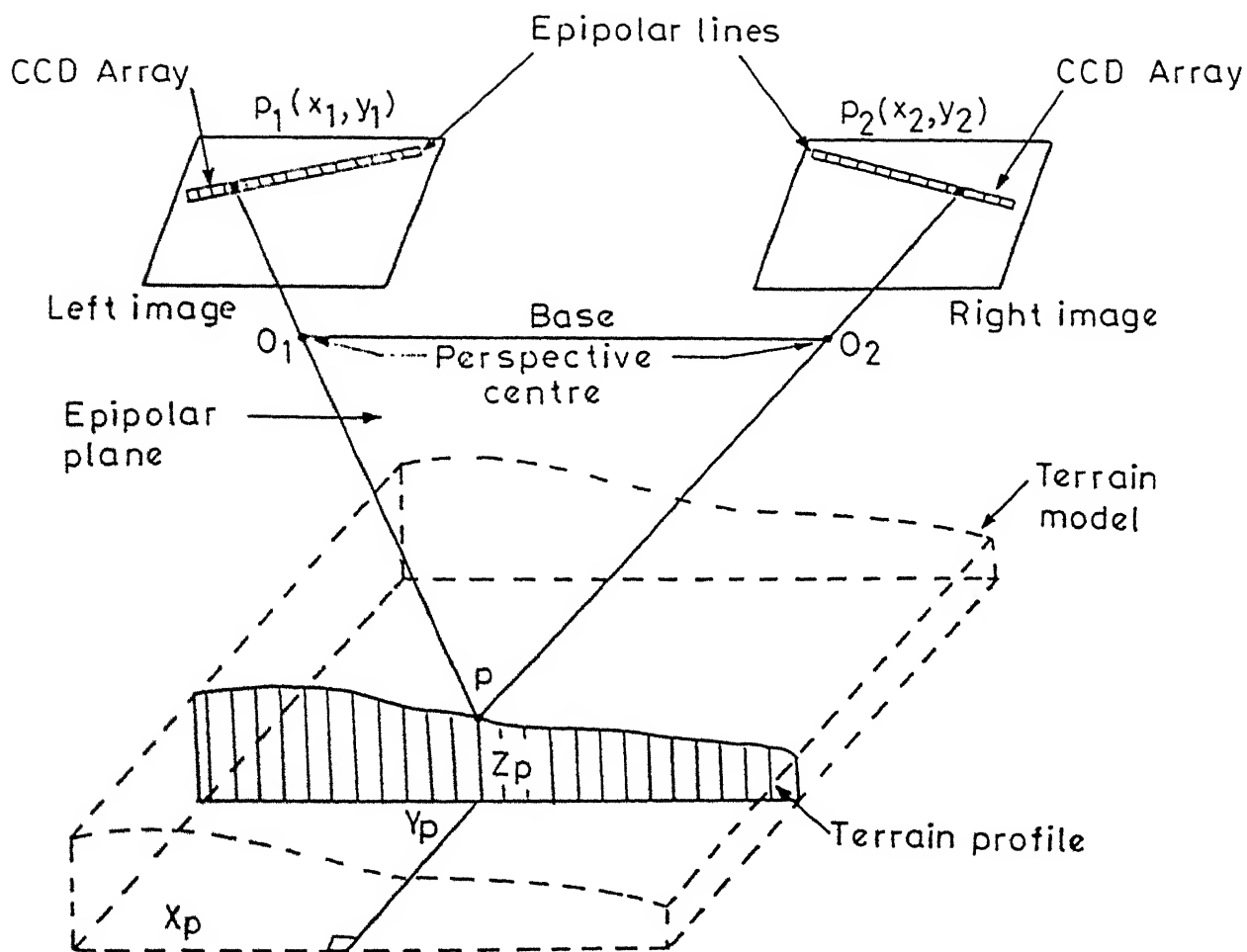


Figure 2.1 Epipolar Geometry
(source: Kennie and Petrie, 1990)

2. Graphics digitizing methods in which the contours shown on existing topographic maps are digitized i.e. converting into strings of digital co-ordinate data and the elevation data is derived from them.
3. Photogrammetric methods based on the principles of photogrammetry

2.1.1.1 Ground survey methods

In this method, height data is normally acquired using the electronic tacheometers. However, it is also possible to acquire the elevation data using the traditional optical instruments like theodolites and tachcometers, or even surveyor's levels to carry levelling, though hardly with the same speed and efficiency.

The accuracy of the field survey is very high, and they are economical and practical to carry over relatively small areas, for example over a sites planned for building construction, or roads, sports grounds, or quarries. If the need is to generate the height information over large area, then this method becomes uneconomical and time consuming. For large areas, the terrain information will be obtained either using photogrammetric methods or by digitising the contour on existing topographic maps.

2.1.1.2 Graphic digitizing methods

Landscape modelling and visualisation, is normally carried out by digitizing the height information contained in existing topographic sheets. These topographic maps contain very few spot heights or elevations, so in dealing with the extraction of height information from topographic maps contour lines are used, they are recorded as strings of digital co-ordinate data. The actual DTM spot height or elevation data is derived by interpolation from the digitized contour lines. The development of terrain model over large areas is useful in areas like aircraft simulators.

It is apparent that by following the above procedure it is not possible to produce the same accuracy as that results from measurement of spot heights in the field using land survey or

photogrammetric methods. The accuracy of contours is normally found to be one third of that of spot heights measured photogrammetrically (Kennie and Petrie, 1990). The individual spot heights derived by interpolation from such contours will have very low accuracy. However, as long as this limitation (low accuracy) is permissible, the utilisation of this lower quality data is very useful. Many users engaged in preliminary or reconnaissance studies, find this quite adequate for their purpose.

The measurement of contour lines is normally carried out manually using a solid state tablet digitize on which contour is traced by using a cursor around which a field coil is placed. This produces a signal which can be picked up by the measuring wires embedded in the tablet which give the x and y co-ordinates of the successive positions measured along an individual contour. This method definitely requires a digital image processing system for registration of map data to image and also to support the digitize. The enormous cost of the systems precludes their use by the surveyors or civil engineers.

2.1.1.3 Photogrammetric methods

The generation of DTM data by photogrammetric methods is generally carried out using stereo plotting instruments. Certainly, there is no other method of survey which will generate the required data about the terrain surface in the form of plans, maps, elevation models, profiles and contours in a timely and economic manner as is required for the planning of all large civil engineering projects. Photogrammetric methods are sub divided as manual or automatic on the basis of execution of the system.

2.1.2 Stereo plotting instruments

The methodology in all stereo plotting instruments involves the use of a pair of overlapping photographs or imageries to form a reduced scale three dimensional model of the terrain. This type of model can be either optical or mechanical in nature. Measurement (or) calculations based on a model constitute an analogue process where the object (the terrain) being measured is simulated by another physical system (the optical or mechanical model) which is measured instead. The instruments which carry out those processes are

called analogue instruments. In analytical type of photogrammetric instruments the solution is purely mathematical and the model is wholly numerical.

2.1.2.1 Optical projection instruments

The instruments of this type comprises two identical projectors with the same geometric characteristics (format size, focal length, angular coverage) of the camera which took the photograph. An optical projection system is shown in Figure 2.2. Positive copies of the pair of overlapping photographs covering the area of interest are placed in the two projectors and are illuminated from above so that the images are projected downwards into the space below the projectors. The two photographs are set in the same relationship to one another as they were at the time of exposure. This is carried by the process of relative orientation in which the operator rotates and shifts the two projectors in a systematic manner, when this is performed correctly the two bundles of corresponding ray from each projector will meet in the space below the projectors and forms an optical model of the terrain. This optical model is viewed stereoscopically (in three dimensions) by the user, and measurements can be carried out on this model which relate directly to the actual height.

The measurements on the stereo model of the terrain are carried out accurately using a free moving measuring device. This device is used to plot a map from the stereo model, the correct position being given by a plotting pencil located directly below the mark. As the ground rises or falls, the measuring mark is continuously adjusted by the observer to the correct height in the model. The measuring mark can be set to a predetermined height and the observer can keep the mark continuously in contact with the optical model of the terrain at that height, producing a plot of that particular contour on the map sheet.

2.1.2.2 Mechanical projection system

The main concept of mechanical projection systems is to duplicate mechanically all the optical components of the projection type of instruments. The mechanical stereo plotting

instrument is shown in Figure 2.3. In optical projection systems, there were photographs, projection lens, projected rays and an optical model. In the mechanical projection system, each photograph is duplicated mechanically as the mechanical photo planes, the projected rays by space rods; the projection lenses are duplicated mechanically as the centre of free moving gimbal system; and the specific point where a pair of intersecting optical rays would meet is the position where the space rods meet and form the mechanical model point.

The term mechanical applies only to the projection or measuring system. It is still necessary for the observer to view the photographs optically and stereoscopically for the height measurements. This is carried out by a mechanical linkage which ensures an correspondence between what is measured and what is viewed in three dimensions by the operator using the instruments optical system. The instruments optical system is to meet the basic requirement that the left eye see the left photo only and the right eye, the right photo only. In this way the operator can view and measure the model of the terrain stereoscopically.

The actual measurement of the mechanical model can be carried out by the operator using a free moving measuring device same as that used in optical projection system. The model generated is a correctly scaled representation of the terrain, the heights measured in this model relate directly to the actual positions and heights present in the terrain.

2.1.2.3 Analytical photogrammetric instrumentation

This is an alternative and increasingly important type of photogrammetric instrumentation system. This system is based on the use of analytical procedures which are purely numerical models based on the mathematical solutions which are implemented in programmed computers. There are several alternative ways in which these solutions may be implemented in practice. From the instrumental point of view, these may be classified mainly into three groups:

1. The use of a comparator as the measuring device and the execution of the analytical solution as an off-line process carried out later in a computer.

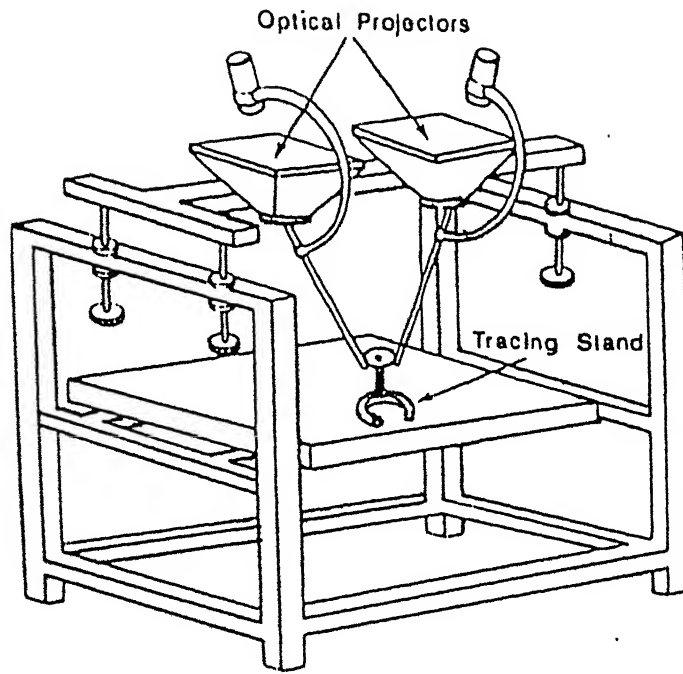


Figure 2.2 Optical stereo projection instrument
(source: Kennie and Petrie)

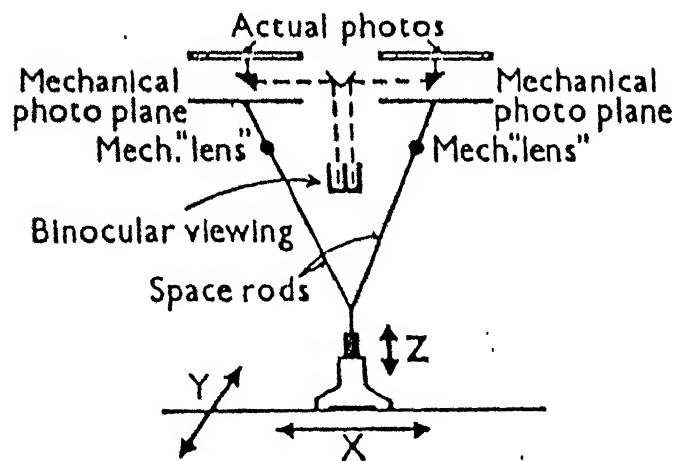


Figure 2.3 Mechanical stereo projection instrument
(source: Kennie and Petrie)

2. The use of a comparator but with the numerical computational solution executed as an one-line process and
3. The construction and operation of an analytical plotter in which the computer is totally integrated into the design of the instrument and the solution is an on-line process, executed in real time and resulting in a continuously oriented stereo model.

1. Comparator and off-line solution

The basic arrangement is shown in Figure 2.4. The measuring device may be a mono comparator or an stereo comparator. In a mono comparator the individual photographs (of a stereo pair) are measured separately. The x, y image co-ordinates of each point are measured with the help of instrument using digitizers and then recorded in a computer compatible form. After the corresponding points on the second photograph of the stereopair have been measured the two sets of measured co-ordinate data can be merged to implement the analytical solution. The use of a mono comparator always results in a off-line computational solution because the height determination takes place separately and sequentially on the individual photos of the stereopair. If the measuring instrument is a stereo comparator, stereo viewing is possible and the image co-ordinates can be measured simultaneously. Later, the numerical solution is implemented to determine the terrain (or height) co-ordinates of all the points.

2. Comparator and on-line solution

The basic arrangement is shown in Figure 2.5. In this the compactor is attached on-line to a computer. The basic measuring process and computational procedure is the same as that of the off-line solution. This arrangement allows the model to be formed and the terrain co-ordinates to be calculated as soon as the minimum number of points needed to implement the analytical solution has been measured. Once this is achieved, the measurement of height at additional points will be completed automatically. In this stereo compactor is having an advantage over the moon compactor.

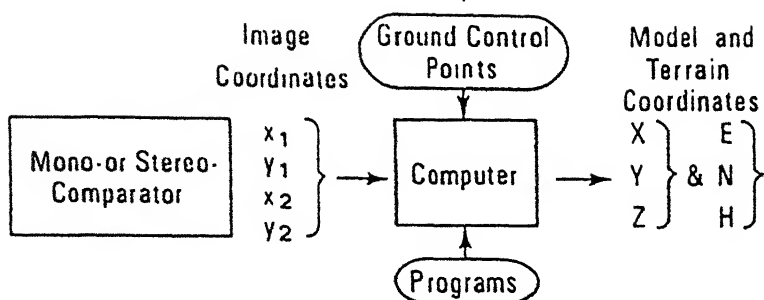


Figure 2.4 Flow chart of comparator and off line solution
(source: Kennie and Petrie)

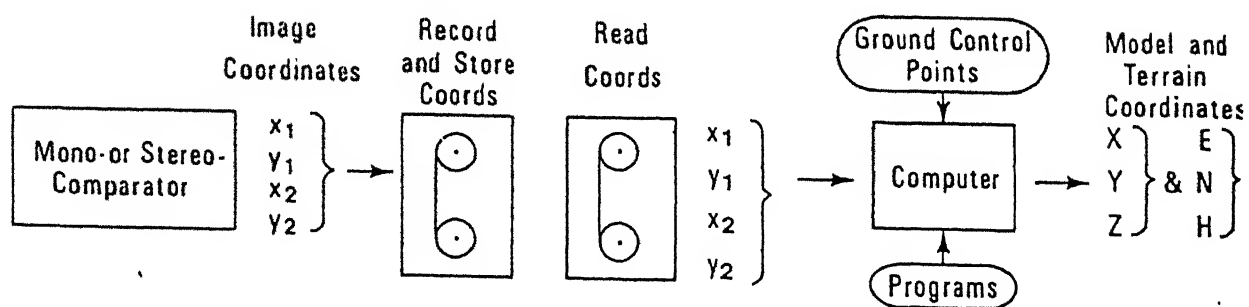


Figure 2.5 Flow chart of comparator and on line solution
(source: Kennie and Petrie)

3. Analytical plotter

In this type of instrument, the computer will always be attached on-line to the measuring elements of the instruments which will be similar to a stereo compactor. The analytical plotter will also feature a closed-loop system in which the computer provides a real time solution of the analytical photogrammetric equations, which is used in adjusting the plates to required positions. This results in an oriented stereo model which is continuously maintained and the measurement can be carried in the same manner as in an analogue stereo plotting instruments.

2.1.3 Stereo matching methods

There are three methods through which stereo matching can be performed. They are:

1. Area-based matching
2. Feature-based matching
3. Hybrid method.

2.1.3.1 Area-based matching

In this method the correspondence of different points is determined by evaluating the similarity of areas around each pixel. In order to evaluate the similarity of areas around points of interest there are two kinds of techniques :

- (i) based on use of correlation function to determine a correlation coefficient which gives the correspondence between the two imageries, and
- (ii) based on iterative least squares algorithm.

2.1.3.1.1 Matching based on the correlation coefficient

In this method a correlation coefficient is computed for each pixel (m, n) of the search area corresponding to the target area pixel. The process is illustrated in the Figure 2.6. The correlation coefficient is determined by applying a mathematical function between points in target areas and in corresponding sub windows of the search area. The size of

the search window (selected from right image) is chosen such that it does include the corresponding point (selected from left image) for which it is looking for. The choice of the function depends on the required accuracy, as well as on computational requirements.

The most widely used function is the classical cross-correlation function $r(m, n)$, with reference to the target and search area it is defined as,

$$r(m, n) = \frac{\sum_i \sum_j (g_t - \mu_t)(g_s - \mu_s)}{\left\{ \left[\sum_i \sum_j (g_t - \mu_t)^2 \right] \times \left[\sum_i \sum_j (g_s - \mu_s)^2 \right] \right\}^{1/2}}$$

where, i and j are span window sizes, g_t and μ_t denote the grey level at (i, j) and its mean in the target area and g_s and μ_s are the grey level and its mean is the corresponding sub window of the search area. This function yields values normalised between 1 and -1; 1 indicates complete similarity, 0 means no similarity and -1 shows opposite similarity. This method is computationally faster and gives good precision of height values.

Another suitable function derived from the consideration of coherent optics is,

$$I(m, n) = \frac{\left\{ \sum_i \sum_j \cos [p(g_t - g_s)] \right\}^2 + \left\{ \sum_i \sum_j \sin [p(g_t - g_s)] \right\}^2}{(MN)^2}$$

other parameters mean same as described above M and N are the size of the target window. Values of this coefficient range between 0 and 1. Where p , the normalisation parameter, is given by

$$p = \frac{0.5\pi (MN)^{1/2}}{\left\{ \sum_i \sum_j (g_t - \mu_t)^2 + \sum_i \sum_j (g_s - \mu_s)^2 \right\}^{1/2}}$$

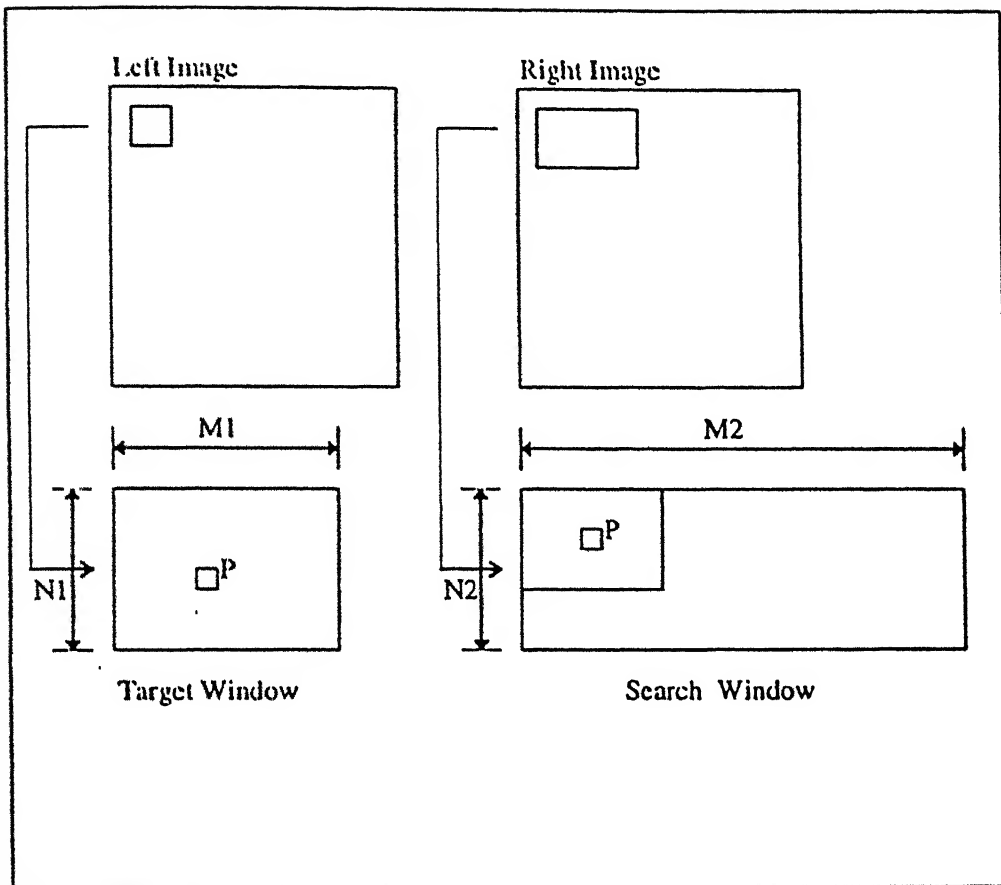


Figure 2.6 Area-based parallax matching principle
(source: Rao *et al.*, 1996)

This method is comparatively computationally slow because of the presence of the mathematical functions in the equation, for which the software has to call those library functions from header file.

Another simple function is to measure the absolute difference between grey levels. This function can be defined as,

$$d(m,n) = 1 - \frac{\sum_i \sum_j |g_i - g_s|}{MNL}$$

where L is the maximum number of grey levels of the image. The value of coefficient varies between 0 to 1. But the accuracy of this function is very less, but computationally very fast (Cappellini *et al.*, 1991).

2.1.3.1.2 Matching based on least squares

This algorithm is based upon mathematical model regarding the target area as obtained through a geometric and radiometric transformation of the search area. Justification lies with in the fact that both $g_t(x, y)$ target area grey level intensity and $g_s(x, y)$ source window grey level intensity represent approximately same object. The above concept can be expressed as,

$$g_t(x_t, y_t) + n(x_t, y_t) = g_n(x_n, y_n)$$

$$x_n = f_1(x_s, y_s)$$

$$y_n = f_2(x_s, y_s)$$

$$g_n = f_3(x_s, y_s)$$

where x_s and y_s represent the position of pixel in the search area; x_t and y_t in the target area; $g_s(x_s, y_s)$ and $g_t(x_t, y_t)$ the grey levels of the search and target area respectively; $n(x_t, y_t)$ is noise. Geometric transforms are denoted by x_n and y_n , while g_n denotes the radiometric transformation. The simplest transformation model without radiometric parameters is,

$$x_n = x_s + p_1$$

$$y_n = y_s + p_2$$

$$g_n = g_s$$

where p_1 and p_2 represent the shift factors. Such parameters can be evaluated by means of an iterative least square procedure (Rosenholm, 1987).

2.1.3.2 Feature based matching

In Feature based matching the images are pre-processed to reduce the noise. The two images are assumed to be in epipolar plane to simplify the matching algorithm. The block diagram for the feature-based stereo method is shown in Figure 2.7. The processing of image enhances the grey level discontinuities (edges). Edges can be easily detected by processing the images with circular operators (sobel operator). Through thresholding and thinning the contours of the scene can be enhanced. The discontinuities (gaps) in the edges are filled by linking with segments of solid lines. This is very important phase for the success of matching procedure.

Proper choice of features such as contrast and orientation allows one to extract from images a complete representation of their information content. Now matching of both the segments of a scene object, both single and grouped, are carried. The remaining procedure is same as that of the area based matching.

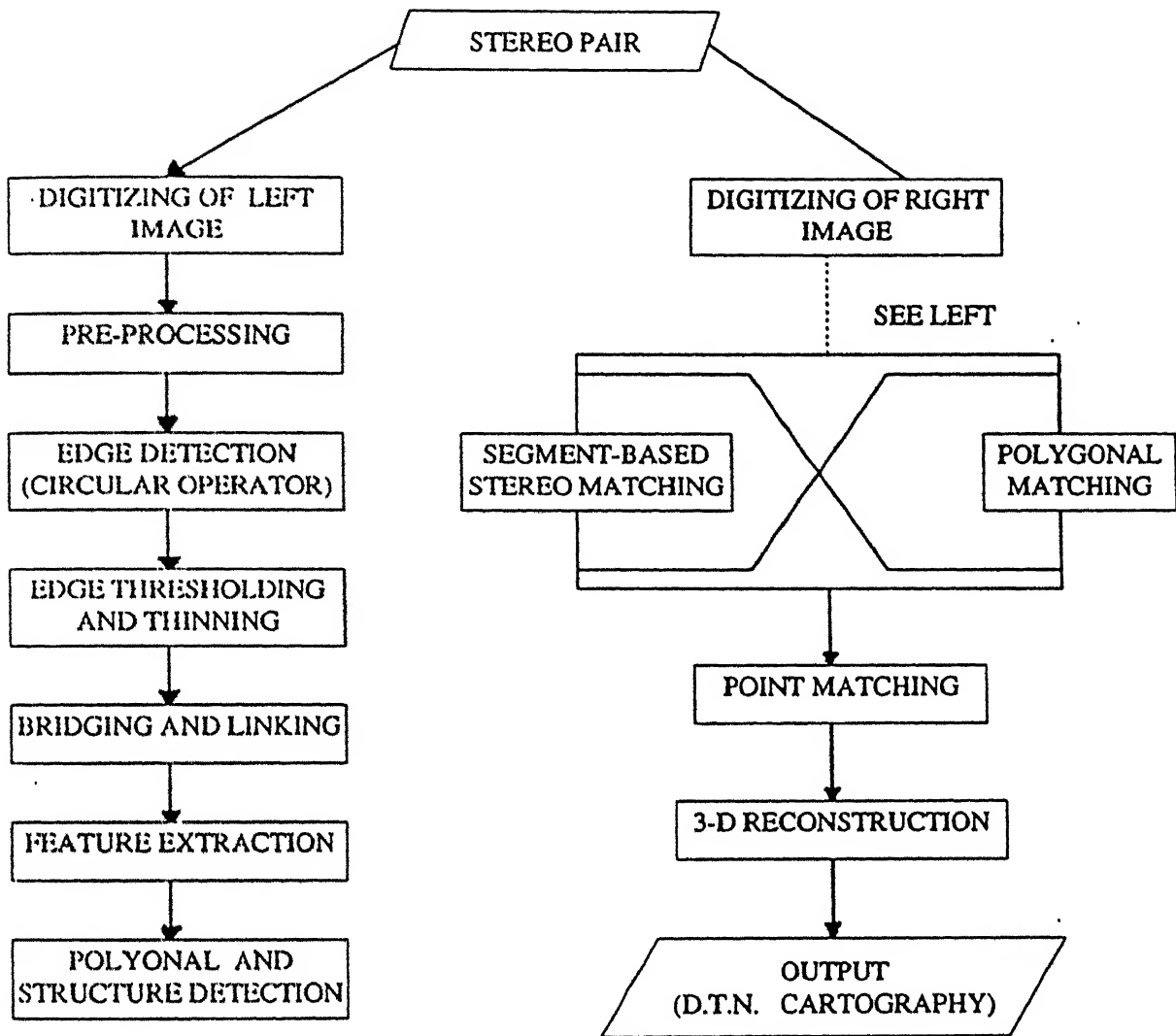


Figure 2.7 Flow chart for feature-base stereo matching
(source: Cappellini *et al.*, 1991)

2.1.3.3 Hybrid model

Hybrid model is implemented as a two-stage process. The feature-based model and area-based model are used in turn in the hybrid model. The feature-based model is used to predict match locations for the area-based model. The area-based model starts as it normally would, but, when the matching grid is constructed, the feature matches are used to form match prediction polynomials. This information from feature-based matching helps the hybrid model find matches quicker (Brockelbank, 1991). The drawback with this method is that any error made by the feature matcher will be repeated in the hybrid model.

2.2 Satellites with Stereo Data Capability

Satellites with stereo data capability were launched in early 1980s. SPOT is the first satellite to be launched (in 1986) with stereo data acquisition facility. In 1996, IRS-1C the first Indian satellite with stereo capability is launched with this facility. The spatial resolution of IRS-1C PAN is much superior to SPOT-PLA. Some of the salient features of these satellite are discussed in brief

2.2.1 SPOT

The SPOT (Système Probatoire d' Observation de la Terre) satellite is designed by the French Centre National d' Etury Spatial (CNES) under the French National Space Program, in association with Sweden and Belgium. The first SPOT satellite is incorporated with two identical High Resolution Visible (HRV) range instruments. These instruments are pointable in the across track direction ($\pm 27^{\circ}$) in order to have access to any point on the globe and for the acquisition of stereoscopic image pairs from different satellite passes (Figure 2.8).

The fundamental architecture is divided into two main parts (Chevrel *et al.*, 1981):

1. "Platform" this carries mission independent sub systems: attitude and orbit control, power supplies, on board computer, telemetry and command equipment, etc.,
2. "Payload", this includes instruments and other mission specified equipment.

2.2.1.1 SPOT mission specifications

1. Complete equatorial coverage capability using the two-sensor system in a fixed, nadir looking operating mode;
2. To have access to any point on the globe, which makes possible for observing designated areas more frequently than possible with nadir view only;
3. Acquisition of stereo pairs over a very short span of time;
4. High ground resolution;
5. Spectral bands to be good indicators of vegetation and species discrimination.

To meet the above requirements, the first SPOT satellite includes two identical High Resolution Visible (HRV) instruments. The HRVs are designed to achieve:

1. a multispectral capability with a ground sampling interval of 20m;
2. a spatial resolution of 10m in panchromatic range;
3. a cross tracking pointing system to provide accessibility;
4. a bit rate of 25 megabits/second/data channel and
5. a radiometric resolution of 256 grey levels (8-bit coding in multispectral mode, red (.50-.59 μm), green(.61- .68 μm), blue(.79- .89 μm)).

The HRV instruments scan ground without any mechanical moving parts, images are scanned by using the pushbroom scanning mode. With pushbroom scanners the exposure time for each ground point is maximum. For the HRV with 20m resolution, an array of 3000 detectors per spectral band are provided, data is sampled at every 3 milliseconds, while for one with 10m ground resolution, the array consists of 6000 detectors per line, data is sampled at every 1.5 milliseconds. Detectors are composed of charged coupled device (CCD) detectors (Chevrel *et al.*, 1981).

LATERAL STEREOSCOPY PRINCIPLE

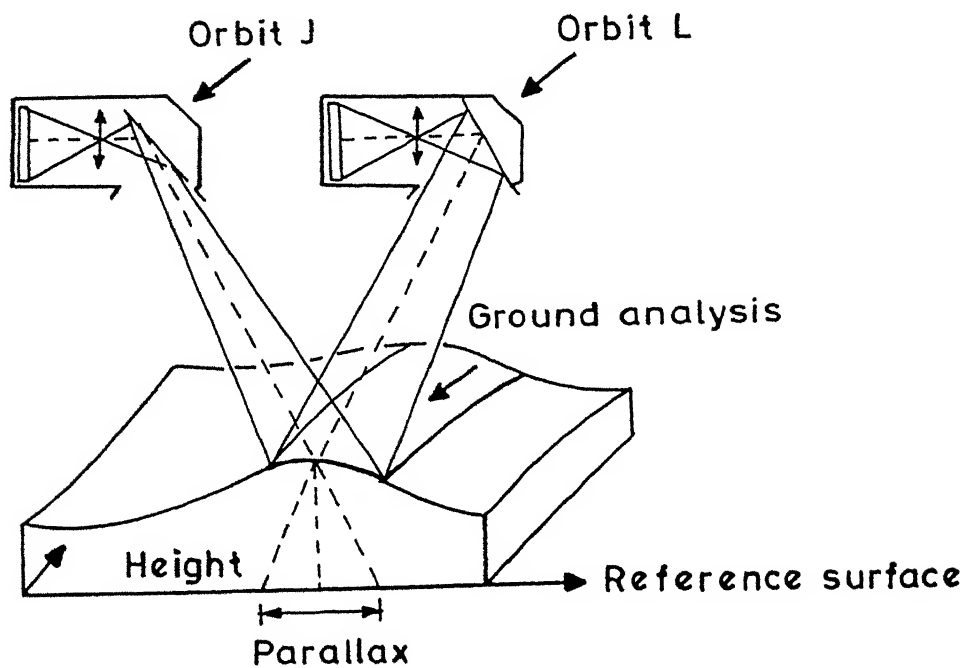


Figure 2.8 Stereoscopic scanning process of SPOT

(source: Chevrel *et al.*, 1981)

2.2.1.2 Stereoscopic ability of SPOT

Stereo images are one which nearly consist of same area but scanned from two different positions. In SPOT, stereo images are obtained by oblique viewing capability, which makes it possible to acquire stereo images by viewing the terrain at different angles during different satellite passes on neighbouring tracks (Figure 2.9). The base to height ratio can reach even one, which is considered as excellent for extracting terrain information. This ability in combination with the high ground resolution of panchromatic mode scanner gives very good precision for cartographic projects.

2.2.2 IRS-1C

IRS-1C is the first Indian Satellite having the capability of providing digital stereo data. This operates in a circular, sun synchronous, near polar orbit with an inclination of 98.96° , and at an altitude of 817 km in the descending node. This is launched with the mission of implementing and managing the satellite data for earth resource survey with advanced sensor capabilities. The architecture of IRS-1C consist of a Main Platform (MPL) and a Payload Platform (PPL). These two incorporate mainframe sub-systems like power, telemetry, tracking and command, attitude and orbit control sensors. The satellite carries three different imaging sensors, which are characterised by enhanced resolution and coverage capabilities. Panchromatic (PAN) camera has an spatial resolution of 5.8 metre. This has an off-nadir viewing capability of $\pm 26^\circ$ which is used to acquire stereoscopic data of terrain. The spectral range of this band is 0.5 - 0.75 μm and is made of three charged couple devices of 4096 elements each. These provide an total coverage of 70 km on ground. Linear Imaging Self-Scanner -III (LISS-III), is a multispectral camera and operates in visible and near IR spectral bands with spatial resolution of 23.5 metres and the short wave IR (SWIR) band is having spatial resolution of 70.5 metres. These cameras are made with 6000 CCDs with interference filters in front. The spectral bands are 0.52-0.59 μm , 0.62-0.68 μm , 0.77-0.86 μm and 1.55-1.7 μm for SWIR (2100 CCDs). Wide Field Sensor (WIFS) is sensitive in visible and near-IR region with a spatial

resolution of 188.3 meters and a swath of 810 km. This is made of 2048 CCDs, with the spectral ranges of 0.62-0.68 μ m and 0.77-0.86 μ m.

2.3 Earlier Works on DTM Generation

Although activities in digital terrain model have started late after stereo satellites have been launched, yet good amount of work is done in this field. Both area-based and feature-based matching methods are thoroughly used. A brief account of works carried in this fields are reported here. Cappellini *et al.*, in 1991 studied the problems involved in the reconstruction of three dimensional profiles which are related to the definition and resolution of suitable equation set for the calibration and to estimate match confidence. Both area-based and feature-based matching techniques were used. They experimented on aerial stereo imageries digitized with a resolution of 50 μ m from the aerial stereo pair. Epipolar geometry was established by parametric method. In determining the parallax, area-based stereo matching methods were considered. In their work comprehensive analysis on the match percentage with respect to correlation coefficient method and target window sizes is performed. Unitary time requirements for each method for different target window sizes were also determined. In their analysis, if the sub pixel accuracy value determined exceeded half the size of the pixel, then that value was discarded. The results for percentage of match points (N_{mp}) and corresponding total standard deviation (S_{xy}) of the errors are shown in the Table 2.1. They suggested that among all the stereo correlation matching methods, cross correlation method is the best, and the sub pixel precision can be achieved by complete geometric affine transformation (six parameters), and by a two parameter radiometric transformation of the grey levels.

Brockelbank and Tam (1991) worked on techniques used to extract accurate elevation information from SPOT stereo images. Both feature-based and area-based stereo matching and hybrid algorithms were used to generate height information at two different test sites. The three stereo models were created as similar as possible to allow comparisons between the models. They used eight manually collected point positions along with satellite ephemeris data to estimate the satellite parameters. The SPOT images are brought into epipolar geometry by using cubic polynomial equations to model the

vertical and horizontal disparity with the help of match control points from stereo images and common co-ordinate positions of those points. The Dinosaur National Monument (DNM) test site images are having inclinations of 11.3^0 for left image and -20.8^0 for right image which gives a base-to-height ratio as 0.58. The root mean square (RMS) error x, y, z in registration of images at test points is 12.8, 13.3 and 11.7 meters. For Red Deer (RD) test area the inclinations of the images are 25.2 for left image and -26.2 for right image, which gave a base-to-height ratio of 0.97. The RMS error x, y, z in registration are 8.5, 9.6, 8.2 meters. The results of the two test areas are shown in Tables 2.2 and 2.3. The better accuracy at Red Deer is due to the superior ground control and satellite parameters. They suggested that area-based matcher performed best among the three methods and feature-based matching performed least. This they attributed to the edge detection process and also to the matching stage, because of the discrete features.

Ehlers and Welch, in 1987, developed DTM from Landsat TM images for rugged terrain area in north Georgia. The stereo data is obtained from the path overlap of the satellite. The base-to-height ratio is found to be 0.18. They establish the epipolar geometry by non-parametric method. In this they used single degree polynomial equation. In this process they considered 13 ground control points, the RMS error for planimetric error values are from $\pm 22\text{m}$ to $\pm 25\text{m}$ for five with held ground control points. The parallax values are determined using area based stereo matching method. They checked the accuracy of DEM by three methods: (1) analysis of Z-error at with held check points; (2) comparison of contour lines derived from the Landsat TM DEM with contours interpolated from the reference map and from existing USGS DEM; (3) pixel-by-pixel comparison of the TM and USGS DEMs.

In first method, height error at seven with held check points yielded an RMS height error value of $\pm 42\text{m}$. This value corresponds to about ± 0.3 pixel. In second method contours of 100m interval were compared, which yielded an RMS height error values of $\pm 33\text{m}$. In third method, the histogram of differences of DEMs yielded a mean value of 5.5m and a standard deviation of 39.0m.

Table 2.1 Sub pixel accuracy evaluation for cross-correlation with different target window sizes

Evaluation	3×3	5×5	7×7	9×9	11×11	13×13	15×15	17×17
N_{mp}	52	64	52	54	56	46	44	36
S_{xy}	0.35	0.33	0.35	0.31	0.32	0.35	0.33	0.33

Table 2.2 DNM DEM Error (RMS meters)

Test points	Feature-based model	Area-based model	Hybrid
26 match test points	16.8	12.1	12.7

Table 2.3 Red Deer DEM Error (RMS metres)

Test points	Feature-base model	Area-based Model	Hybrid model
58 match test points	10.1	8.52	8.90
15 map test points	8.84	7.45	7.95
29 Alerberta Land Survey	8.46	4.55	4.82

Rao *et al.*, in 1996, used the overlap area between the two adjacent paths of IRS LISS-II as a stereo pair for the generation of DTM. The spatial resolution of LISS-II of IRS-1A is 36.25 m. The orientation of the images into epipolar geometry is performed by non-parametric method. This process is carried using first order polynomial equations. The planimetric RMS error was found to range between 10m to 15m. Parallax is determined by using area-based method in which cross correlation stereo matching method is used. Absolute DTM is generated from relative DTM by using 12 GCPs absolute terrain elevation. This observed that 90 percent of RMS error fall within 33.95 m in Palghat test area, 34.45 m in Pune and 38.12 m in Dehradun on 30 map test points.

2.4 Chromo-Stereoscopy

This is a technique of depth perception, developed by Toutine and Rivard in 1995. Einthoven proposed the Chromo-Stereoscopy theory in 1885. In this phenomena, the colour objects present on the same plane appear at different depths. In positive chromo-stereopsis the objects with red colour have higher apparent elevation in comparison to objects with blue colour, while opposite sense of colour objects is called negative chromo-stereopsis. Einthoven proposed that this phenomena is due to the chromatic dispersion and relation between the visual and optical axes. It is possible to enhance the chromo-stereopsis by controlling the refractive properties of the material used in making lenses. The amount by which the light refracts when it passes from one medium to another is completely dependent on the speed of the light in those medium. The speed of the light is depend on the wave length of light. The division of a white light into different colours when it passes through prism is a good example of this concept.

The basis concept in generation of the chromo-stereoscopic image is to classify the depth present in the image by means of assigning colours, and decoding the coloured image by means of special optical instrument. In the process of generation of these optical instruments glasses made with prisms (plastic, glass, fresnel) worked extremely well, but the production of such instruments on large scale is found to be uneconomical. Later

research community experimented with thin diffractive optics. These lenses incorporate a high precision system of micro optics. When light passes from one medium to another it produces differential angular parallax by virtue of its dependence on the refractive index value of the material and wave length of light. An example of this is shown in Figure 4.1. When light passes through single prism glass, it is subjected to deviation. This deviation of light makes the object to appear much closer to the eyes (shown in Figure 4.2.a). This gave rise to two major problems (Steenblik, 1986,1991):

1. because of this deviation of light rays, the object appears to be shifted from the focal point of the eyes. This causes strain to the eyes.
2. While looking at the object if the user changes his position, the object moves differently from what the brain anticipates. This results in visual disorientation of the sight.

To rectify both the above mentioned problems, double prism glasses are used, this pushes the object back to the position at which it was supposed to appear (shown in Figure 4.2.b). The two prisms used, a low dispersion and a high dispersion are designed in such a way that the deviation of yellow light is zero, and the other colours are deviated with respect to their wave lengths. Because of the high dispersion prisms, red objects appear at higher level than the objects having blue colour.

CHAPTER THREE

METHODOLOGY AND RESULTS

As mentioned earlier, the generation of digital terrain model mainly involves following steps:

1. digital stereo pair acquisition from the satellite,
2. establishing the epipolar geometry,
3. parallax computation using stereo correlation techniques, and
4. relative and absolute digital terrain model computation.

The flow chart for computation of DTM is shown in Figure 3.1.

3.1 Digital Stereo pair acquisition from satellite

The first step in the generation of digital terrain model is acquisition of data, in this thesis SPOT stereo satellite data is used. Data is supplied by NRSA, Hyderabad. In stereo pair each image is of 1024×1024 pixels. The left image is having an angle of 18.0004° and the right image is having an angle of -2.4° . Left image intensity values ranged from 22 to 101, whereas the right image intensity values ranged from 23 to 93. Images were acquired in April, 1993. The base-to-height ratio calculated is 0.3668. Stereo images are shown in Figure 1.4.

3.2 Establishing Epipolar Geometry

A pair of digital images has been obtained for the test area. They have been scanned from two different points of view. The first step to be performed is the establishment of an epipolar geometry. In the satellite stereo imageries, there are two types of parallaxes, vertical and horizontal. Vertical parallax, generally known as Y-parallax is due to the spacecraft motion in-between the scanning of the stereo pair, and the horizontal parallax,

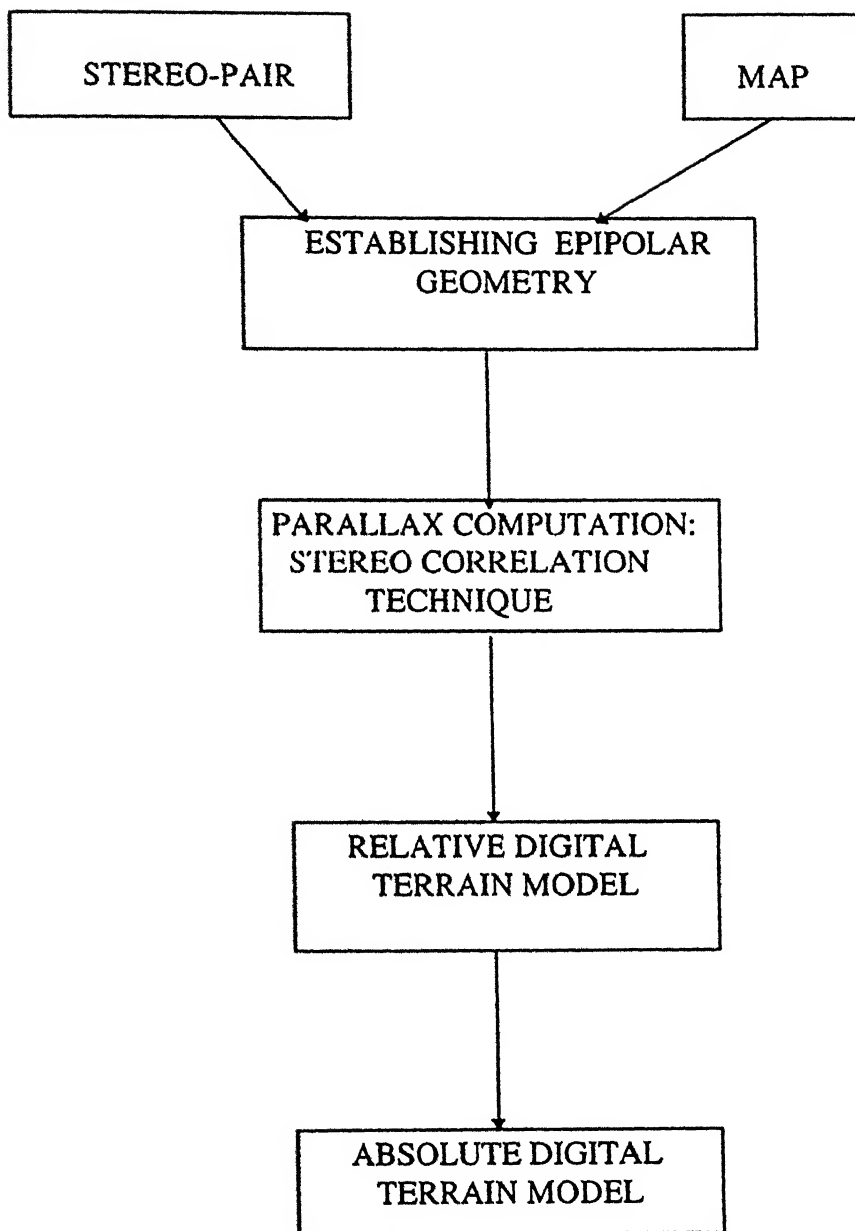


Figure 3.1 Flow Chart for Computation of DTM

known as X-parallax is due to the terrain relief. X-parallax is used in generating height information. Before finding the X-parallax by correlation techniques, it is necessary to align the two images along the horizontal direction as shown in the Figure 2.1. This process is known as establishment of epipolar geometry, which helps in reducing the search area for matching corresponding image points. In order to achieve the epipolar geometry of a stereo pair, either a parametric or a non-parametric approach is used. A non-parametric method does not require the satellite ephemeris (ancillary) data that was recorded during the image acquisition. This approach uses a mathematical function relating image co-ordinates and corresponding ground control points (GCPs) on the map. The establishment of epipolar geometry through a non-parametric approach involves the registration of both the images (stereo pair) on to a common co-ordinate system. This process is known as *geometric rectification*.

3.2.1 Geometric rectification

Two basic operations must be performed in order to rectify a remotely sensed image on to a map co-ordinate system.

1. The geometric relationship between the input pixel location (row, column) and the associated map co-ordinate of this same point (latitude, longitude) must be identified. This will establish the nature of the geometric co-ordinate transformation that must be applied to rectify a image. This procedure is known as *spatial interpolation*.
2. The grey level value in the rectified map has to be determined. There is no one to one relationship between the movement of input pixel values to the output pixel locations. A pixel in the rectified output image may require a value which does not belong to a row and column co-ordinate of the original image. An interpolation has to be carried for this, which is known as *intensity interpolation*.

3.2.1.1 Spatial Interpolation

Both SPOT images are rectified using a first order polynomial transformation. This type of transformation can model, scale translation and rotational distortions. To implement this transformation process, four different polynomial equations must be modelled. They are,

1. x (latitude) as a function of r (row) and c (column) of the image.
2. y (longitude) as a function of r (row) and c (column) of the image.
3. c (column) as a function of x (latitude) and y (longitude).
4. r (row) as a function of x (latitude) and y (longitude).

They can be expressed mathematically as,

$$\begin{aligned}x &= a_0 + a_1 c + a_2 r \\y &= b_0 + b_1 c + b_2 r \\c &= p_0 + p_1 x + p_2 y \\r &= q_0 + q_1 x + q_2 y\end{aligned}$$

In order to solve the coefficients of these polynomial equations, co-ordinate sets of (x, y) and (r, c) of ground control points (GCPs) are used. While selecting a ground control point on a image, two important facts must be considered. One is the ground control point must be clearly visible on image and also identifiable in the topographic map and the second is, the ground control points must be well distributed over the entire image. In mathematical terms, the minimum number of ground control points required for solving the polynomial equation are n , where n is the number of coefficients in the polynomial expression. For a first order polynomial, n is equal to 3. For a second order polynomial n is 6 and for third order polynomial n is 10. These sizes of n are to meet the mathematical needs, but the statistical requirement, which is more concerned with the interpretability and reliability of the results insists on much higher standards. Generally 10 to 15 control points will give acceptable results for a first order polynomial transformation (Rao *et al.*, 1996). In this thesis 14 ground control points are used. The method of least squares regression is used to

find the coefficients of the polynomials. The polynomial coefficient values determination is shown in three steps,

$$\begin{aligned}
 P \cdot a &= E \\
 P^T \cdot P \cdot a &= P^T \cdot E \\
 a &= (P^T \cdot P)^{-1} \cdot P^T \cdot E
 \end{aligned}$$

where

P is a row/ column matrix

E is latitude/ longitude matrix

a is the coefficient matrix

However, before applying the rectification to the entire set of data, it is important to determine how these coefficients accounts for geometric distortion in the input image. The method used involves the computation of the RMS error for each of the ground control point. Let the original row and column co-ordinate of the ground control point be R_{orig} and C_{orig} . The position of the same point is measured from the map. Now using the six coefficients which are used to transform a point from map to image, the corresponding position is calculated, let them be R^1 and C^1 . Logically both R_{orig} and C_{orig} and R^1 , C^1 should represent the same point, any discrepancy in values represent image distortions not corrected by the six coefficients. The distortion is measured by computing RMS error for each control point,

$$RMS\ error = [(C^1 - C_{orig})^2 + (R^1 - R_{orig})^2]^{1/2}$$

User generally specifies a threshold for this RMS error. If on evaluation of the total RMS error (sum of RMS error of all GCPs) exceeds this threshold, delete from analysis the GCPs that has the greatest amount of individual RMS error, and recompute the coefficients. This process continues until the total RMS error is less than threshold or the number of ground control points become too few.

3.2.1.2 Intensity interpolation

Once the polynomial transformation equation coefficients are finalised, the four corners of the image is transformed to map co-ordinates to obtain the position occupied by the image area in the topographic sheet. Next step is to define the box area in which the area is circumscribed. Now with the spatial resolution (of 10m), the area is resolved into pixels with there positions known in toposheet. In radiometric resampling, the pixels of the geometrically rectified (transformed) image grey level values are determined by transformation of map pixel position on to the image, if this (transformed co-ordinates) does not maps to any position in the original image, the pixel is filled with zero intensity. If the transformed pixel co-ordinates maps to a position in image, then any one of the following intensity interpolation method is followed to assign the intensity value.

(i) Nearest neighbourhood technique

This is a zero order interpolation. This simply chooses the pixel that has its centre nearest the point located in the image as shown in Figure 3.2.a. This is a computationally very efficient procedure.

(ii) Bilinear interpolation technique

This is a first order interpolation technique. This uses three linear interpolations over four pixels that surround the point as shown in Figure 3.2.b. Bilinear interpolation assigns grey level value to output pixel by interpolating brightness values along two orthogonal in the input image (shown in Figure 3.2.b). It basically fits a plane to the four pixel values nearest to the desired position in the input image. This process computes the brightness by weighted distances to these points. The closer is the pixel to the desired location, the more weight it will have in the final computation of the average. This method also acts as a spatial moving filter that sub dues extremely high intensity values in the output image. Two

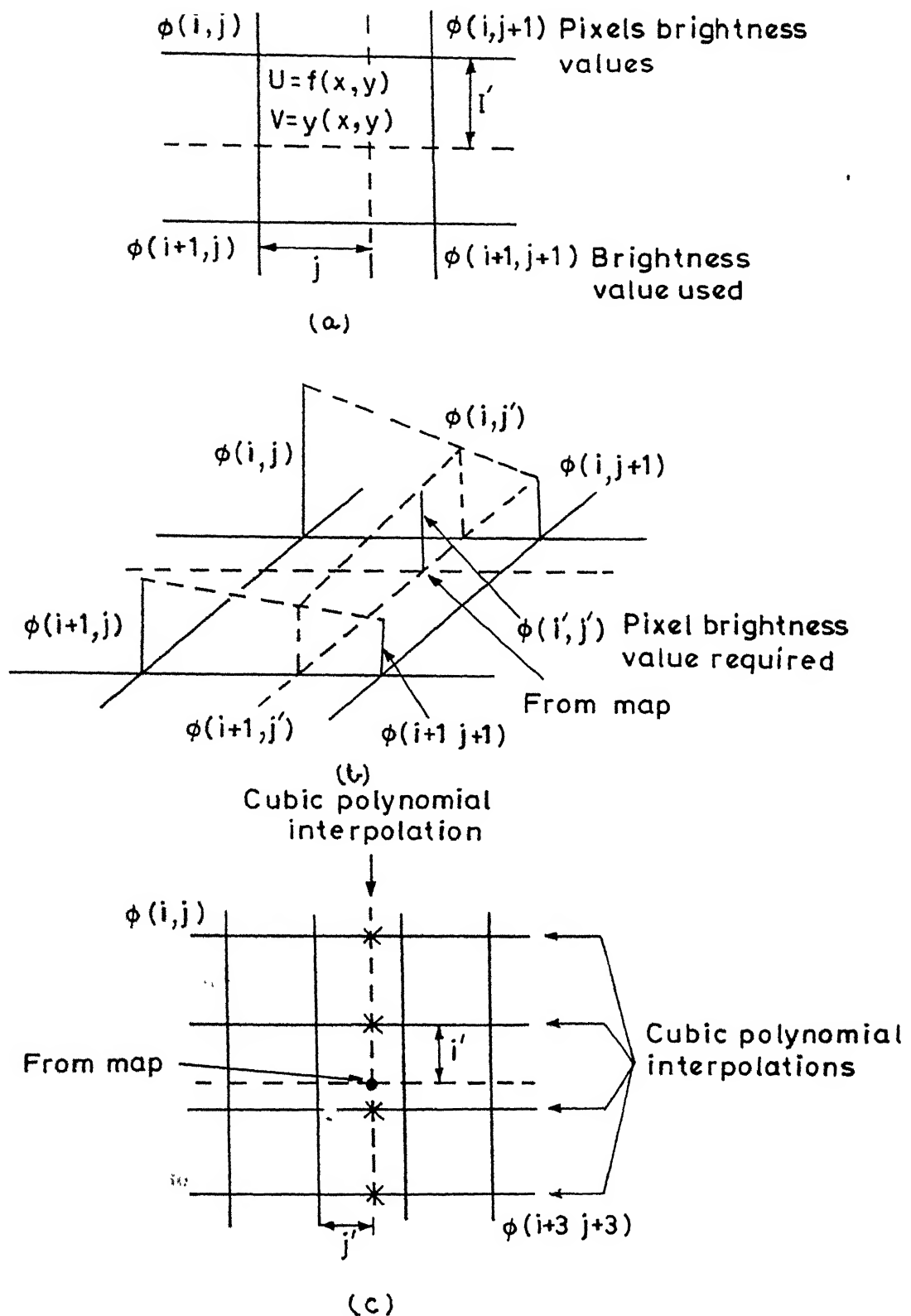


Figure 3.2 Pictorial representation: (a) Nearest Neighbourhood method, (b) Bilinear Interpolation and (c) Cubic convolution.

(Source: Richards, 1995)

linear interpolations are performed along the scan lines to find the interpolates $\phi(i, j^1)$ and $\phi(i+1, j^1)$ as shown.

$$\phi(i, j^1) = j^1 \phi(i, j+1) + (1-j^1) \phi(i, j)$$

$$\phi(i+1, j^1) = j^1 \phi(i+1, j+1) + (1-j^1) \phi(i+1, j)$$

where ϕ is pixel brightness and (i^1, j^1) is the position at which interpolated value is required. The final step is to interpolate linearly over $\phi(i, j^1)$ and $\phi(i+1, j^1)$, which is shown below,

$$\phi(i^1, j^1) = (1-i^1) \{ j^1 \phi(i, j+1) + (1-j^1) \phi(i, j) \} + i^1 \{ j^1 \phi(i+1, j+1) + (1-j^1) \phi(i+1, j) \}$$

This method is computationally more demanding than the nearest-neighbour method.

(iii) Cubic convolution method

This is a second order interpolation technique. Resampling assigns values to the output pixels in much the same manner as in bilinear interpolation, except that the weighted values of 16 input pixels surrounding the location of the desired input pixel position are used to determine the value of the output pixel. Cubic polynomials are fitted along the four lines of four pixels surrounding the point in the image as shown in the Figure 3.2.c. The fifth cubic polynomial is then fitted through these to obtain the required interpolated intensity value $\phi(i^1, j^1)$.

$$\begin{aligned} \phi(i^1, j^1) = & i^1 (i^1 (i^1 [\phi(i+3, j^1) - \phi(i+2, j^1) + \phi(i+1, j^1) - \phi(i, j^1)] \\ & + [\phi(i+2, j^1) - \phi(i+3, j^1) - 2\phi(i+1, j^1) + 2\phi(i, j^1)]) \\ & + [\phi(i+2, j^1) - \phi(i, j^1)]) \\ & + \phi(i+1, j^1) \end{aligned}$$

r 8'

In implementation of this thesis, nearest neighbourhood intensity interpolation is performed. In generating a Digital Terrain Model, parallax or the shift of the position of a point or

pixel is determined by correlation techniques which works with the intensity values of image. In order to maintain the originality of the two images, it is very much needed to maintain the original pixel intensities, which is possible only by nearest neighbour intensity interpolation technique. More over this method is computationally very effective, which helps in reducing the processing time.

3.3 Parallax Determination

Once the stereo images are established in epipolar geometry the next step to be performed is parallax determination. In this thesis area based matching is performed.

3.3.1 Area Based Matching

In this matching process, similarity is determined by correlation coefficient method. In determination of parallax, the right image is radiometrically normalised with reference to its corresponding left image, to have approximately same mean shade as the first image. This can be performed by using the following equation (Rao and Deekshatulu, 1983).

$$g_n^1 = g_n \left(\frac{\sigma_l}{\sigma_r} \right) + \left(m_l - m_r \left(\frac{\sigma_l}{\sigma_r} \right) \right)$$

where g_n^1 is the normalised right image pixel grey value, g_n is the right image input pixel value, σ_l is the standard deviation of the entire left image, σ_r is the standard deviation of entire right image. The mean values of left and right image are m_l and m_r .

As the test area is hilly in nature, with elevations ranging from 550m to 1200m, the maximum correlation points are identified by moving a 11×11 target window in 21×31 search window (as shown in Figure 2.6), allowing a pixel deviation in the horizontal direction and ±3 pixels in the vertical direction. In latter stage, the point of maximum correlation is modified by moving a 7×7 or 5×5 or 3×3 target window in 11×11 search

window. The sub pixel accuracy is computed by using the following equation (Rao and Deekshatulu, 1983).

$$dx = \frac{r(x+1,y) - r(x-1,y)}{4r(x,y) - 2r(x+1,y) - 2r(x-1,y)}$$

where, (x, y) is the position of the maximum correlation and $r(x, y)$ is the correlation value at that point. The calculated parallax file has to be filtered to remove mismatching or noise using a conditional filter.

3.4 DTM Computation

The parallax determined in the above step is used to find a relative DTM (Ehlers and Welch, 1987), using the following equation;

$$d_h(x, y) = d_x(x, y) \times H / B$$

$$B / H = \tan \alpha + \tan \beta$$

where, $d_h(x, y)$ is the relative height at (x, y) ; $d_x(x, y)$ is the parallax at (x, y) ; H is the satellite altitude, B is the air base. α and β are the view angles of the satellite at the time of scanning the terrain which are provided in the header file of the image. The absolute DTM is created by scaling the relative DTM by linear regression techniques with 8 well distributed GCPs of the known height co-ordinates obtained from the SOI topographic sheet of 1:50,000 scale.

3.5 Generation of Height Map

Height map module is developed with an aim to represent the terrain elevation in the form of grey level intensity. The height file obtained by following the above methodology is used as input. Here, the software processes the height file and determines the maximum and

minimum elevation values present in the data. The maximum elevation value is mapped as the highest intensity value, and the intensity values of other elevations are determined by what proportion they are when compared to the maximum height. The output of this process is an grey image with the intensities representing the relief of the area. The number of intensity levels in this image are equal to maximum relief value.

3.6 Generation of Height Classified Map

In this method, classification of the height file is performed. Height file is classified on the basis of the relief value, i.e., height file is divided into different levels of intensities with respect to relief. Each classified level can be given either a colour intensity or a grey intensity value. In general height maps are classified into not more than 8 levels.

3.7 Generation of Solid Model

In generation of solid model, the surface is created by developing polygons. Each polygon created will have elevation proportional to the height value at that pixel. This process is carried at all pixels present in the image, which results in a solid model. In order to better perceive this 3D model, only three faces of the polygon are drawn, which are sufficient to create a solid model. The virtual camera installed in the STARBASE graphics can be rotated from 0° - 360° , which makes it possible to view the terrain model from any direction. The colour of face of the polygons can be altered.

3.7 Generation of Mesh Model

In this module, surface of the terrain is represented as mesh. Mesh is developed by drawing lines from the required points. Mesh surface drawn through all the points will not give the transparent look to the model, because of the large number of points. So the line is drawn through points at regular interval. The colour of surface can be changed. . The virtual camera installed in the STARBASE graphics makes it possible to rotate the model. ~

3.8 Generation of Slope Map

Slope maps are very essential to understand the nature of terrain. This requires the knowledge of terrain, which is supplied in the form of height file. Methodology to generate the height file is already explained. Once this information is obtained, the height file is processed by moving a window to determine the slope at that point. Window size has very significant effect in this process, as the distance used in the calculation of slope is the product of pixel ground resolution and half the window size minus one. If the size of the selected window is large, the resulting slope values will be less in comparison to one with smaller window size. The window operation is shown in the Figure 3.5. The value of height at pixel at which slope is to be determined is obtained by dividing the difference of height value at that pixel from the adjacent pixel height value and dividing it with spatial resolution of the satellite. If the diagonal pixel values are also taken into consideration, the difference value is divided by square root of square of spatial resolution of satellite. This gives the slope at that pixel, this process is carried at all pixel positions to obtain the slope map of the height file. The slope map obtained is less in size by one window size minus one in comparison to height map. This slope map so formed can be classified with respect to the slope value. Generally slope map is classified into six to eight levels.

For four adjacent pixels,

$$s(m, n) = \text{difference in elevation} / 10.0$$

for four adjacent diagonal pixels,

$$s(m, n) = \text{difference in elevation} / 14.14$$

Where $s(m, n)$ is the slope value. Results and discussions of the output data is presented in later part of current chapter.

RESULTS

Once the data is acquired, the second step in the this process is the establishment of epipolar geometry. In the present work it is established by non-parametric method using first order polynomials. Fourteen well distributed points present in both the images are selected for the establishment of epipolar geometry. The row and column numbers of the GCPs are listed in the Table3.1. By using these 14 ground control points and linear regression technique, the six coefficients of the polynomials are determined. These calculated coefficients are tested for their confidence. For left image the total planimetric RMS error for 14 points was 37.86779 pixels, which is very high. This high planimetric error value is due to non availability of good GCPs. From these 14 GCPs the four points with maximum planimetric error are discarded and the coefficients of the polynomials were recomputed, the total planimetric RMS error from the recomputed coefficients is 14.5 pixels. This being also high, three more points with high RMS error are discarded, and the values of the coefficients are calculated, the total planimetric error for these seven points has reduced 6.6 pixels. Further reduction of the total planimetric error is not carried because at least seven to eight points are required for geometric transformation. Because of the non availability of permanent features on the image, some GCPs have been taken along lake and stream, which in combination with time gap between the printing of the toposheet (1988) and the image scanned (1993) could have contributed to this high error. For right image the total RMS planimetric error was 36.39 pixels for fourteen GCPs. From these fourteen points, four points with high RMS error were discarded and the values of the coefficients have been determined. For these ten GCPs total RMS error has reduced to 11.07 pixels. This also being very high three more points have been eliminated. The coefficients of polynomials are calculated using remaining seven points. The total planimetric RMS error from this coefficients is 1.854049 pixels, which is satisfactory.

Geometric correction of the two images is performed using the corresponding set of six coordinates. Radiometric resampling is performed using nearest neighbour method, in order to preserve the original intensity values of the image. Parallax is determined by using area based stereo correlation method. In this, all three correlation coefficient methods discussed before were initially used, but the intensity function and absolute value methods were not giving good results in comparison to cross-correlation method, so the analysis is carried for only cross-correlation method only. Comprehensive analysis is carried with respect to target window sizes varying from 3×3 to 13×13 with respect to their correlation coefficient threshold value. Results of this work are shown in Figures 3.3 to 3.8. Individual time values of each target window size are calculated, graph of this is shown in Figure 3.9. This analysis is very important in digital photogrammetric system as this helps the user in selecting the target window size and the threshold value of the correlation coefficient to required percentage success and the match confidence.

Absolute DTM is generated from the relative DTM by linear regression techniques. In this process 10 GCPs are used. The accuracy of the DTM is determined by comparing the DTM value with 39 map position values. The root mean square of error is 17.46m. Accuracy results are in Table 5.2. The frequency distribution of the error is given in Table 3.3.

This obtained height map file is used in the software package to develop different outputs for better perception of the terrain. First among them is the height map. The height map of the terrain is developed by assigning the pixel positions with grey level intensity values, which are the measure of height at that place to maximum height present. The height map for the present test site is shown in Figure 3.10. Height classified map gives more than a height map. In this one can easily identify the zones of respective sliced areas. The height classified map of the present test site is shown in Figure 3.11. Two different types of surface representation modules are incorporated in this software, a mesh model to show the terrain in transparent mode, and the solid model to give the model a more real time impression. In present software, surface models for small image sizes of range 512×512

pixel are advised to use. This is because when the large image is to be observed camera position has to be located at far distance, from where the user may not fully visualise the terrain variation. The present test site is divided into four parts and surface models are created. Mesh models are shown in Figures 3.12.a to 3.12.d. Solid models of the test area are shown in the Figures 3.13.a to 3.13.d. The slope classified map is one in which the slope of the terrain is divided with respect to its slope present at that pixel. To generate these maps first a slope map has to be generated, which further is used to develop the slope classified map. In present software, slope at a point is determined by comparing the height differences with eight neighbouring pixels (for 3×3 window) with respect to their distances. Slope classified map of the present test site is shown in Figure 3.14. Contours are generated by using GNU plot (a package). The software generates the input file specified by the user and directly accesses the GNU plot to develop the contours/ contours along with surfaces, contours along with surface is shown in the Figure 3.15. The contour plots for the entire test area are shown in Figure 3.16. Another very important depth perception technique provided in this software is the Chromo-stereoscopy. The methodology of which is discussed in Chapter four. In the chromo images generated by compressing the grey level intensities, the sharpness of the image increased with compression of the grey level intensities. The results of the Chromo-stereoscopy are discussed in detail in Chapter Four.

Table 3.1 GCP Positions in Left and Right Images

Number	Position in Left Image row,column	Position in Right Image row,column
1	49, 401	31, 331
2	244, 153	220, 80
3	141, 104	116, 31
4	28, 501	11, 432
5	87, 423	69, 353
6	386, 545	370, 461
7	735, 871	727, 789
8	981, 258	960, 170
9	884, 459	867, 374
10	767, 961	759, 879
11	758, 561	743, 484
12	111, 440	93, 366
13	705, 715	694, 632
14	845, 1000	838, 913

Table 3.2 Elevation error summary at few selected points

Error range	-38m to +35m
position of data sets that agree exactly(%)=	2.5
have negative errors(%)=	40
have positive error(%)=	57.5
root mean square error(m)=	17.46
mean error(m)=	14.256
standard deviation of error(m)=	1.5

Table 3.3 Frequency distribution of errors at few selected points

Range(m)	Frequency(%)	Cum. Frequency(%)
above -30	2.5	2.5
>= -25	5.0	7.5
>= -20	2.5	10.0
=> -15	2.5	12.5
=> -10	13.14	25.64
=> -5	12.82	38.46
=> 0	2.5	2.5
> 0		56.41
=> 5	7.6	48.72
=> 10	12.9	38.46
=> 15	15.3	28.21
=> 20	5.22	7.94
=> 25	5.13	10.25
=> 30	10.26	5.12

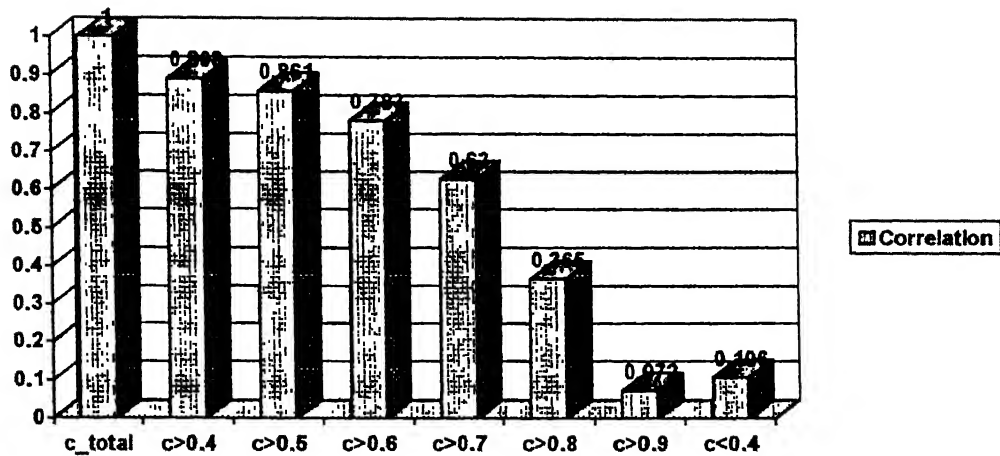


Figure3.4 Correlation Coefficient results for Target Window size 3×3

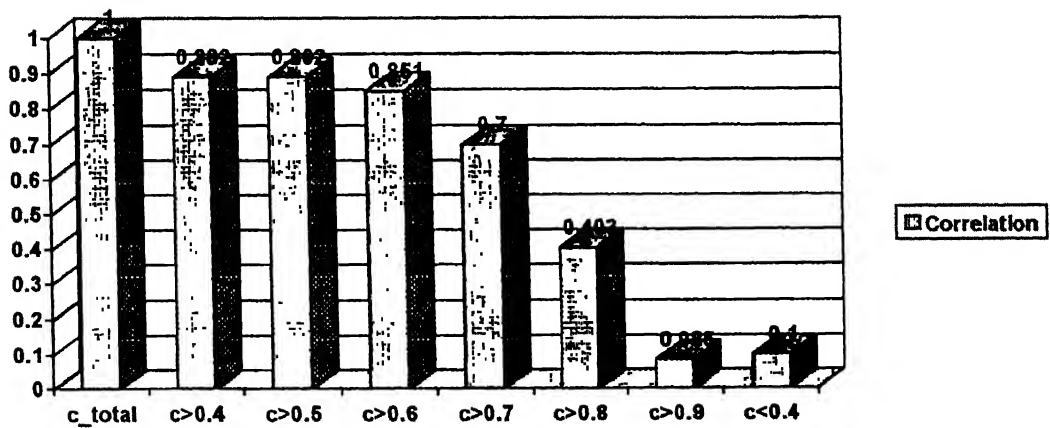


Figure 3.5 Correlation Coefficient for Target Window size of 5×5

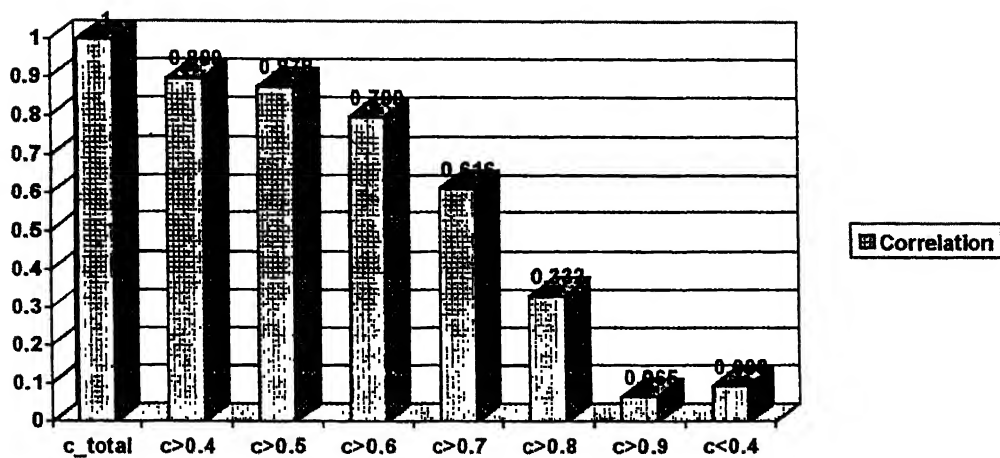


Figure 3.6 Correlation Coefficient results for Target Window size 7×7

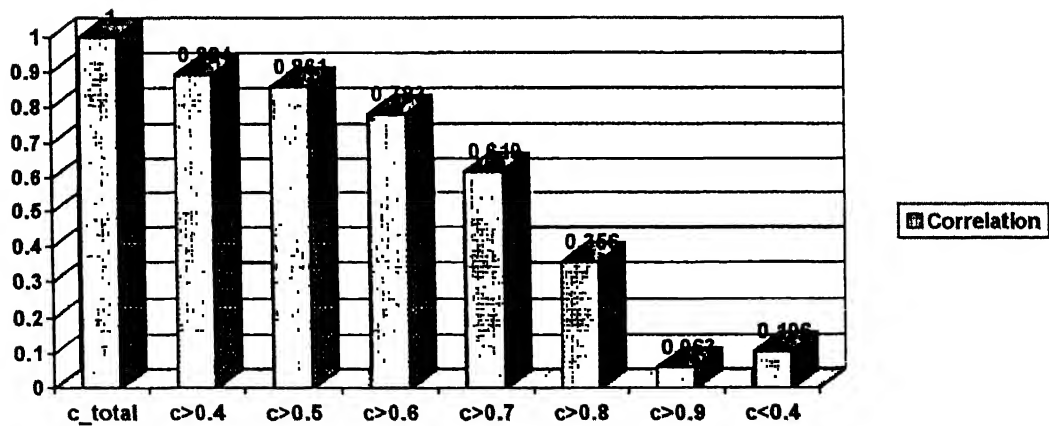


Figure 3.7 Correlation Coefficient for Target Window size of 9×9

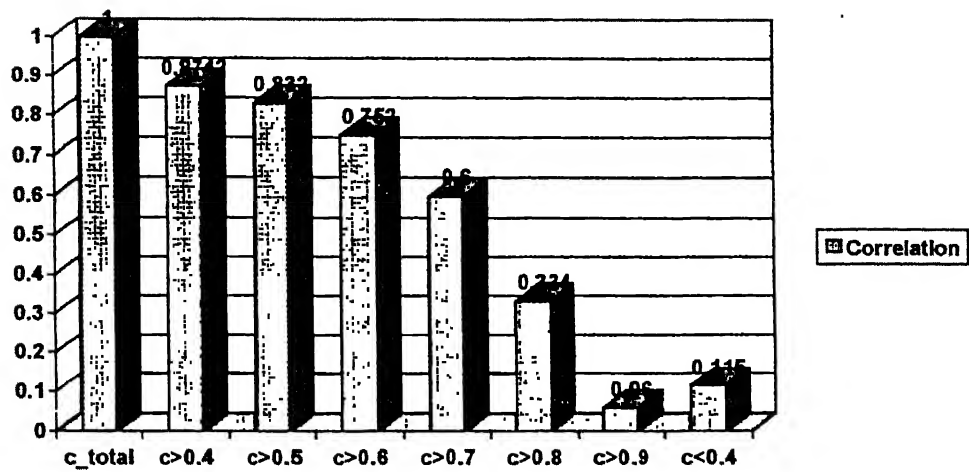


Figure 3.8 Correlation coefficient for Target Window of size 11×11

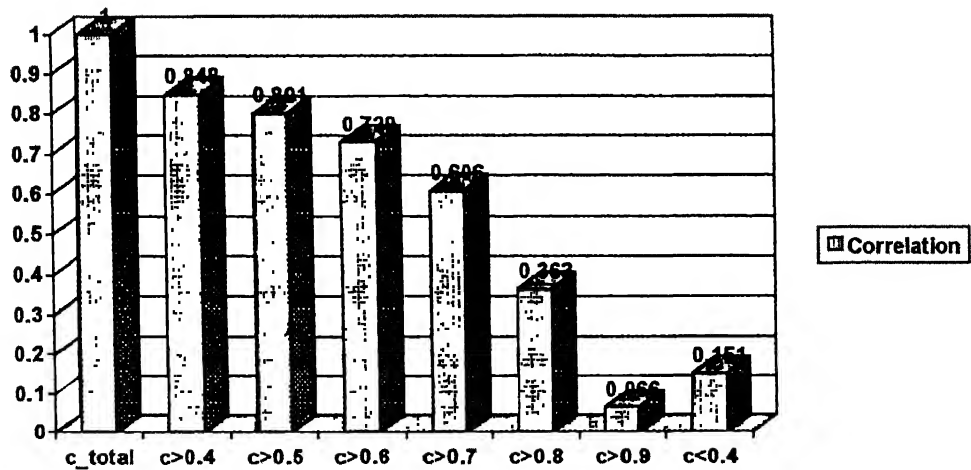


Figure 3.9 Correlation coefficient for Target Window of size 13×13

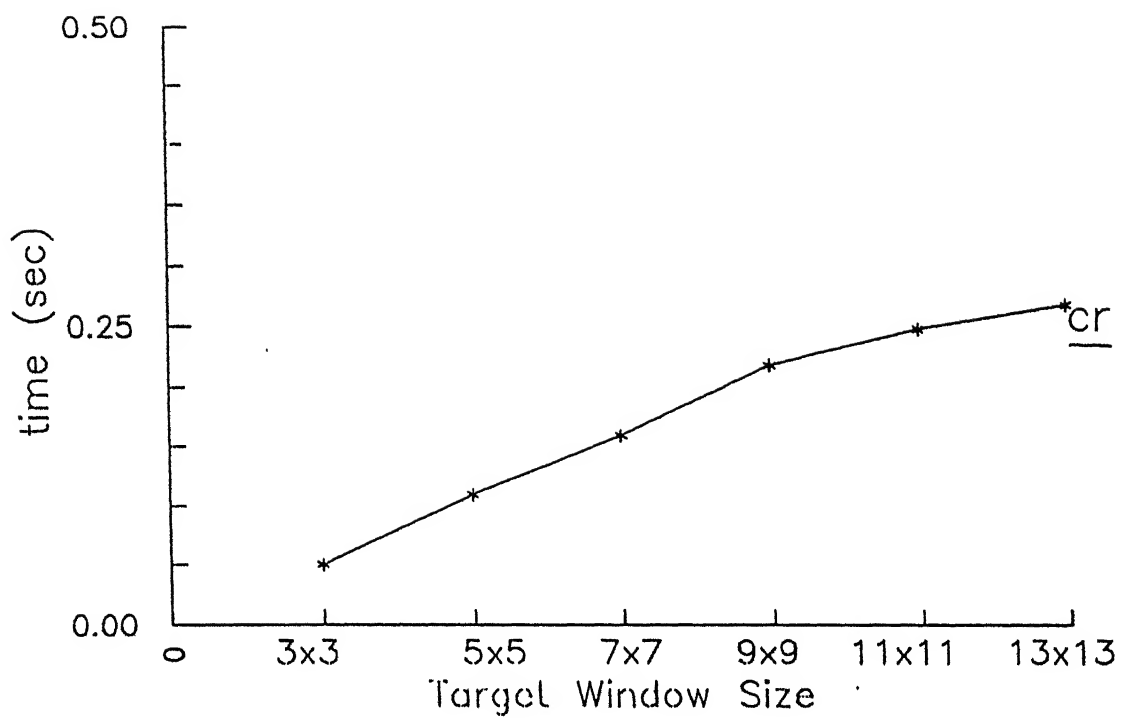


Figure 3.9

Unitary computation time for cross-correlation method

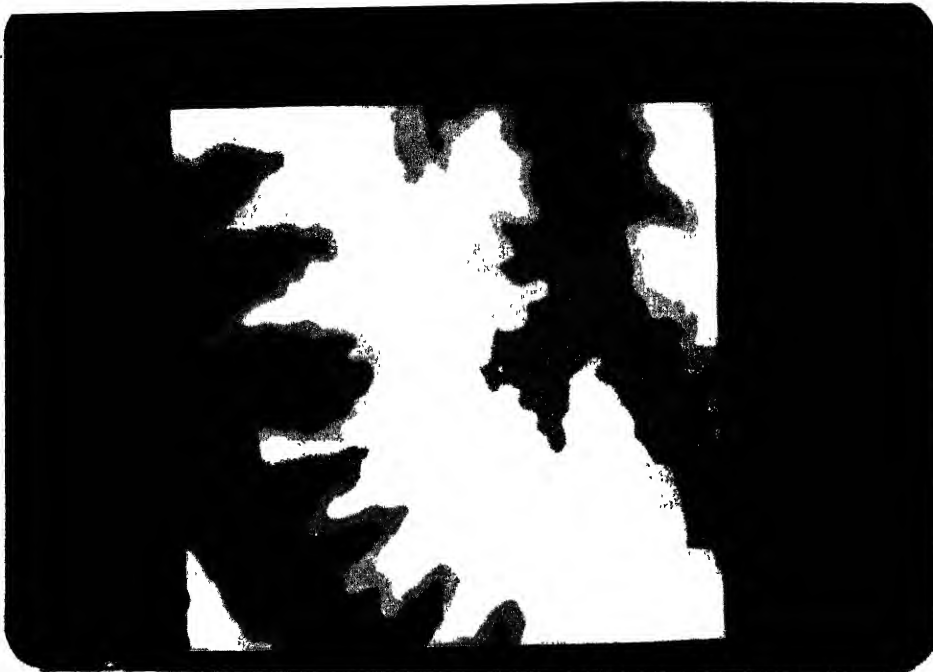


Figure 3.10 Height Intensity Map

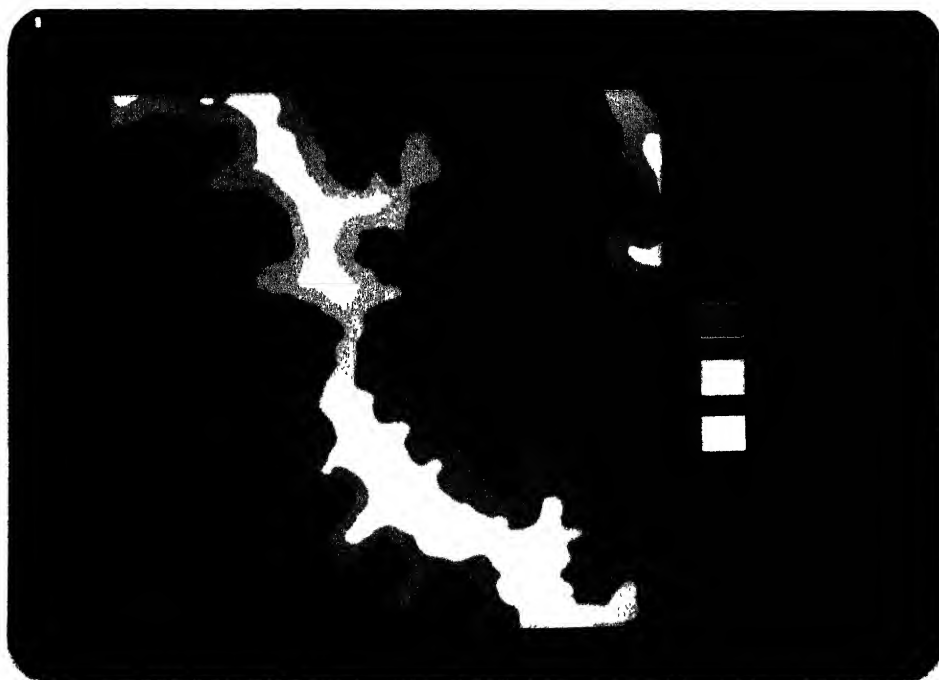


Figure 3.11 Height Classified Map

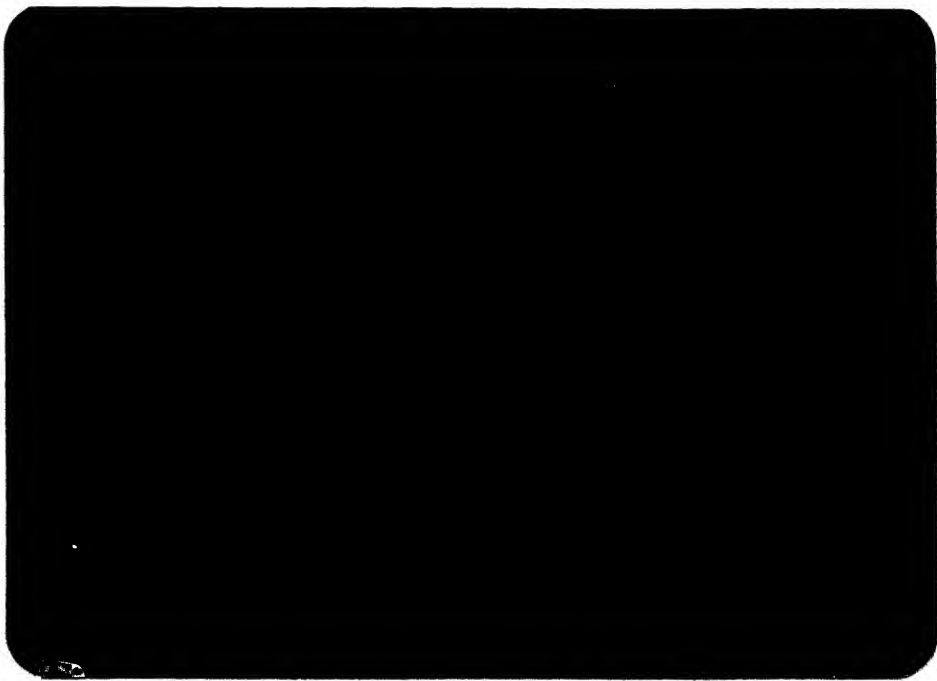


Figure 3.12.a Mesh Model of DTM for Top Left Region



Figure 3.12.b Mesh Model of DTM for Top Right Region

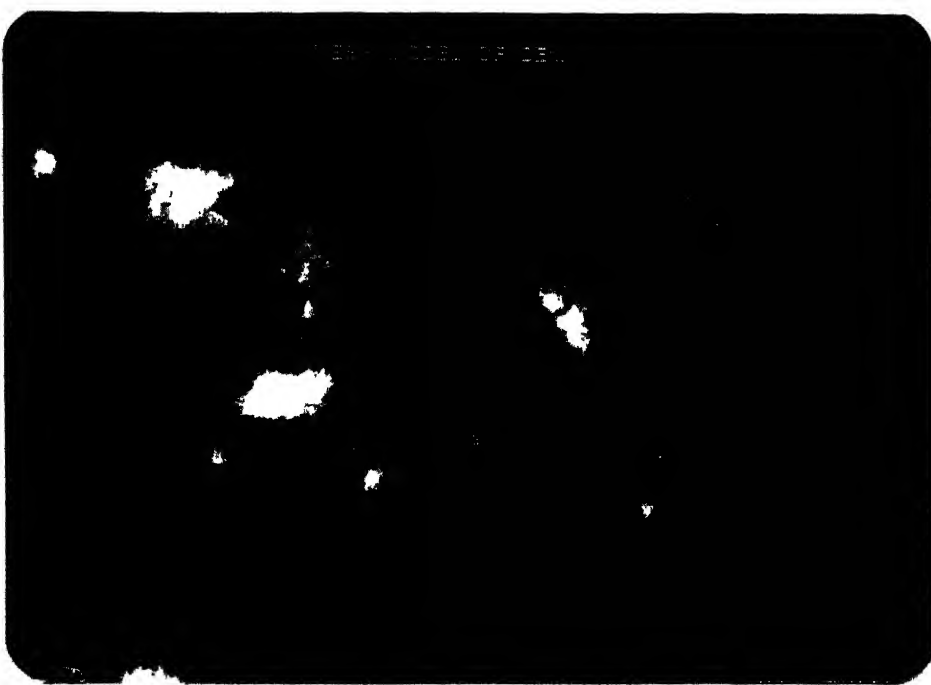


Figure 3.12.c Mesh Model of DTM for Bottom Left Region



Figure 3.12.d Mesh Model of DTM for Bottom Right Region



Figure 3.13.a Solid Model of DTM for Top Left Region

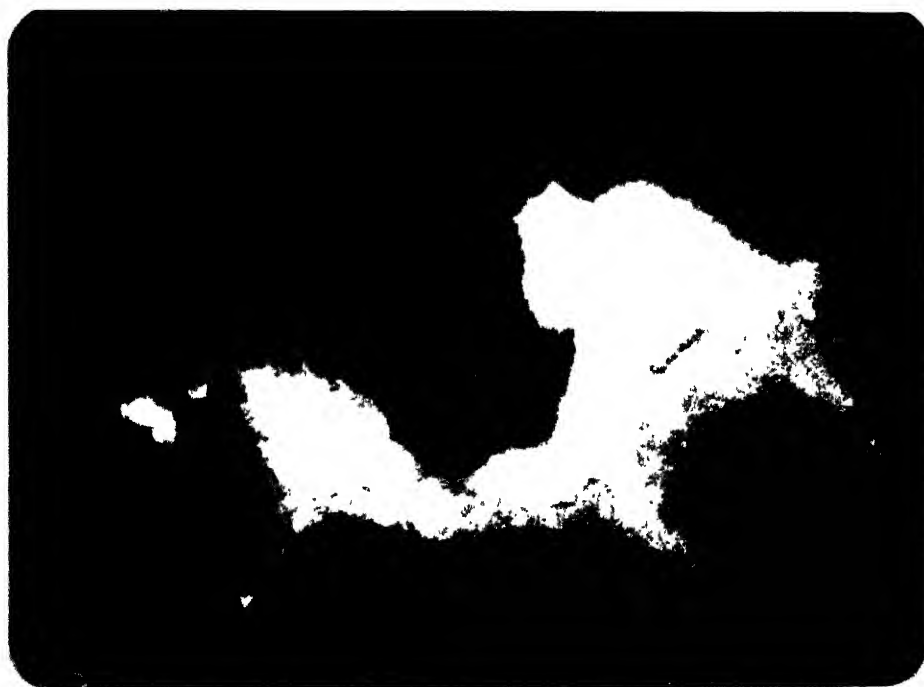


Figure 3.13.b Solid Model of DTM for Top Right Region

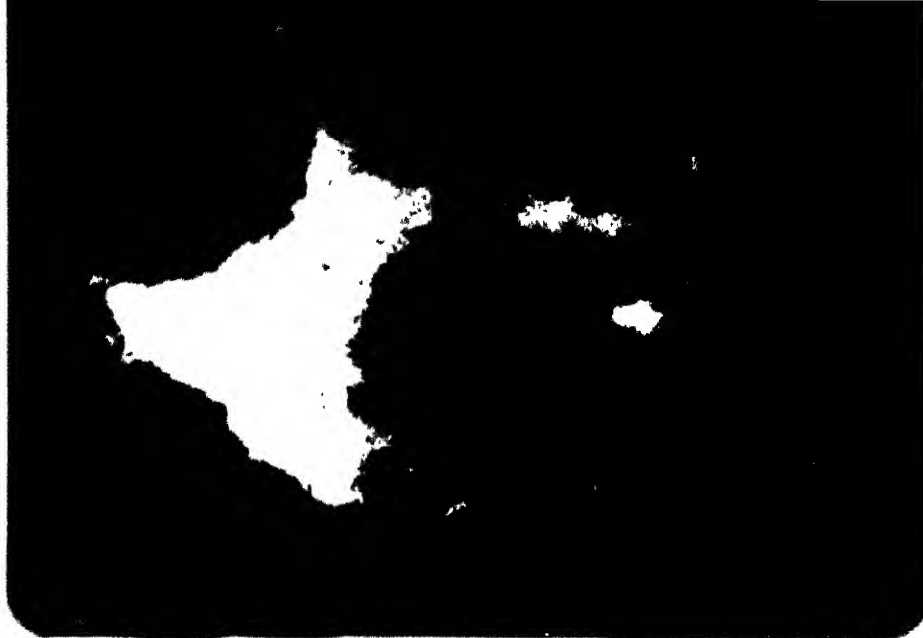


Figure 3.14.c Solid Model of DTM for Bottom Left Region

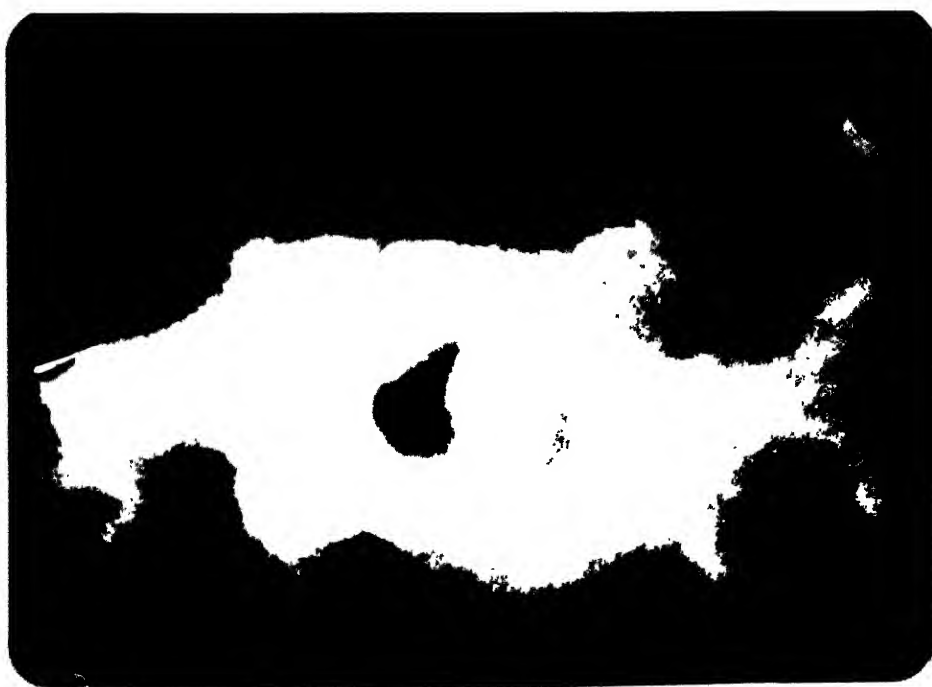


Figure 3.14.d Solid Model of DTM for Bottom Right Region

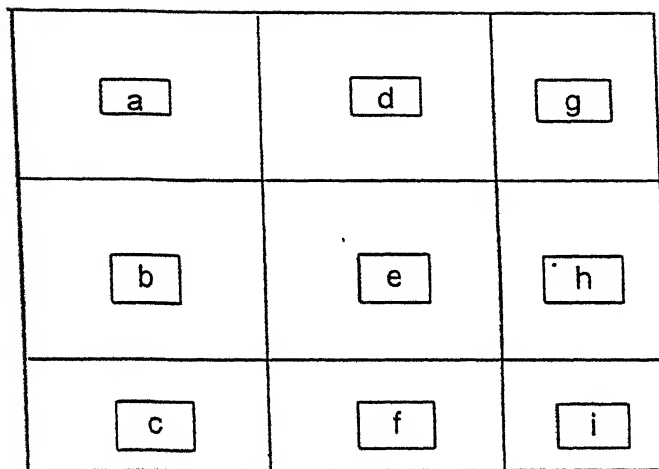


Figure 3.16' Block diagram of contour plots of test area

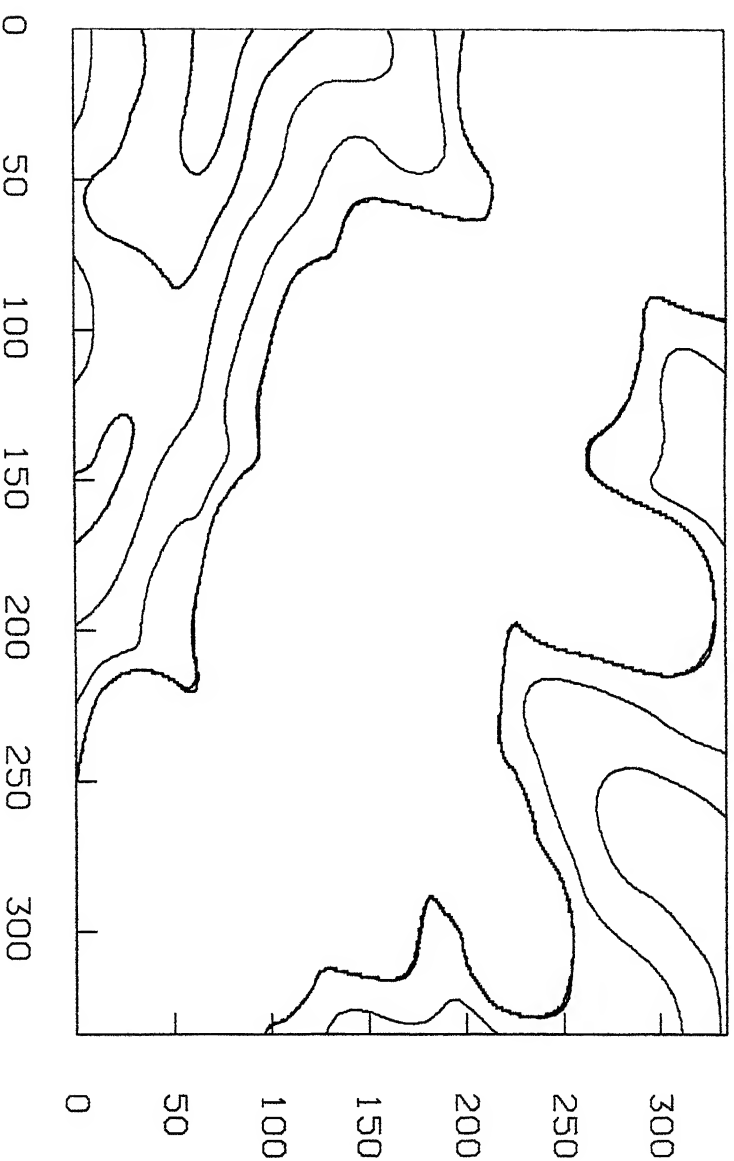


Figure 3.16.a

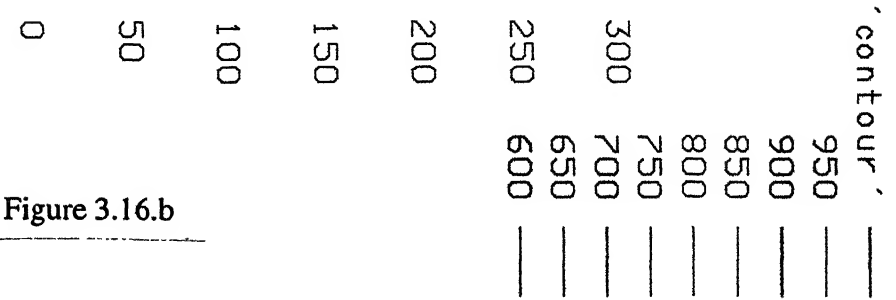
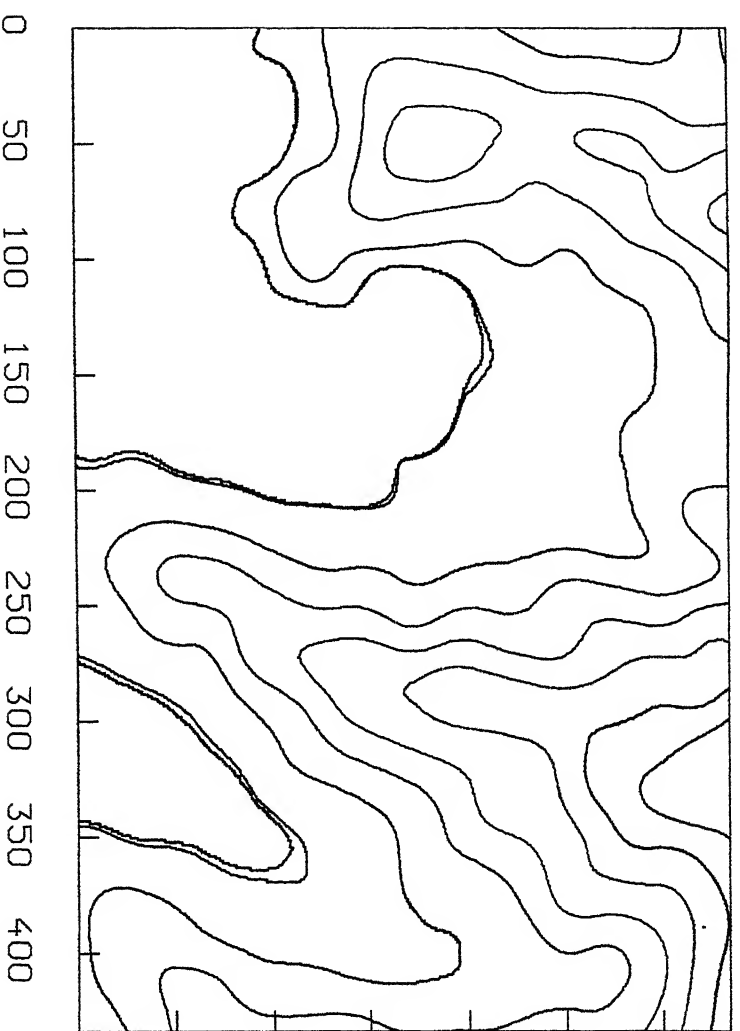


Figure 3.16.b

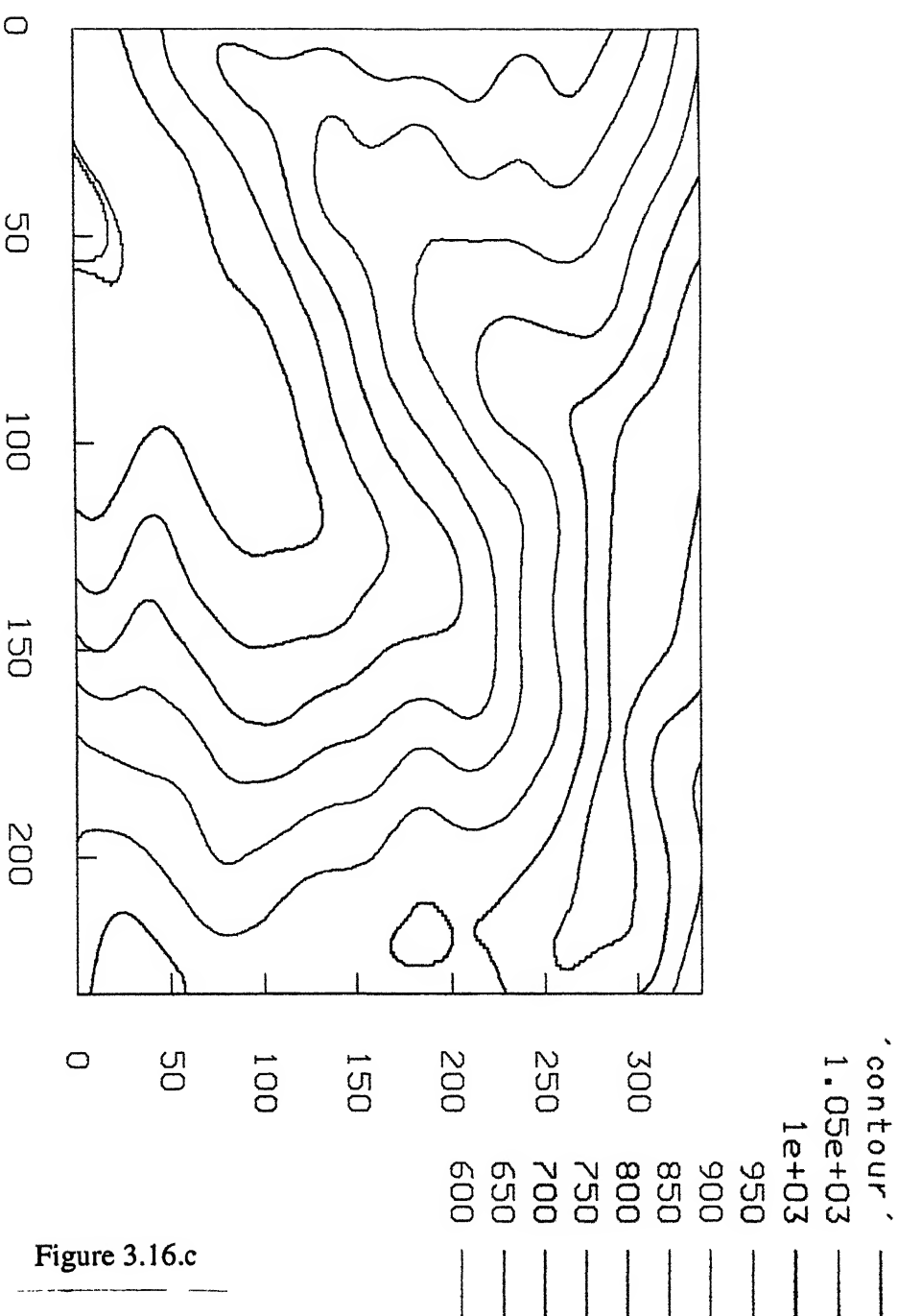


Figure 3.16.c

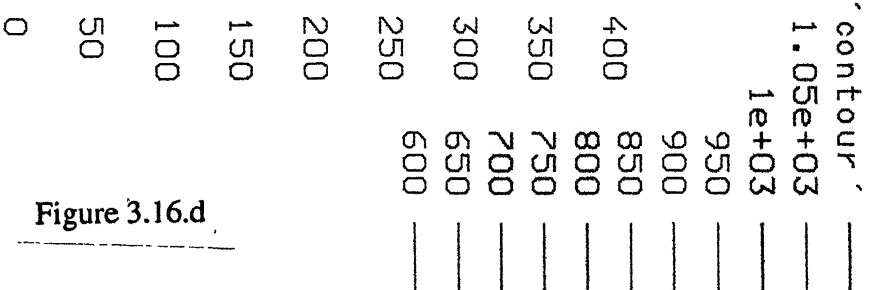
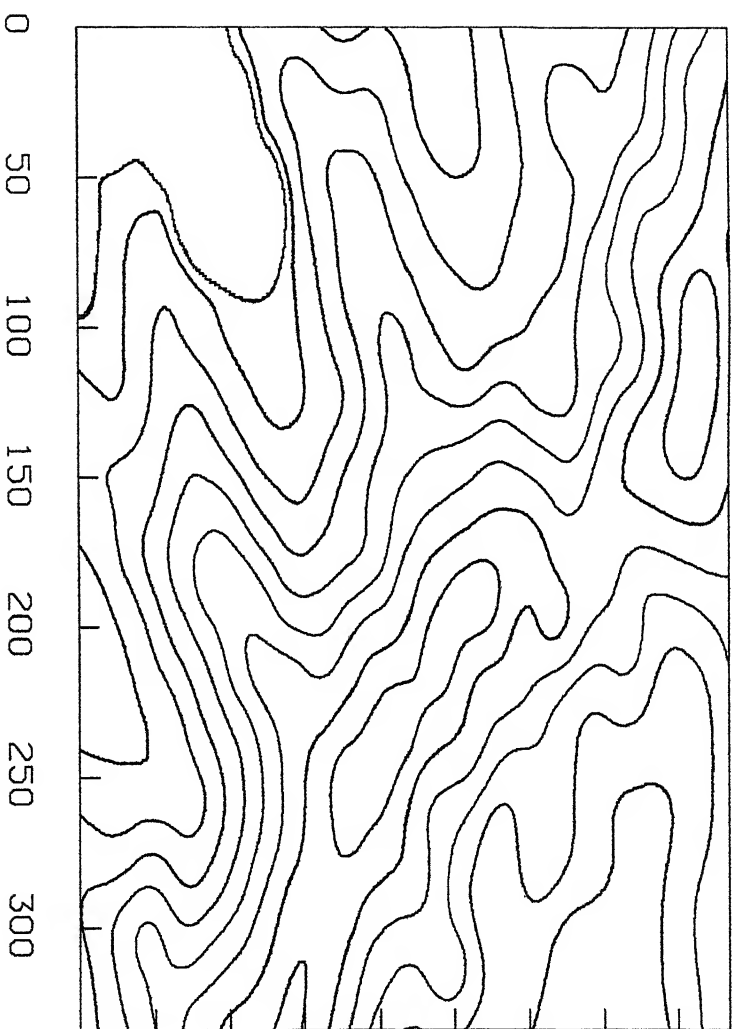


Figure 3.16.d

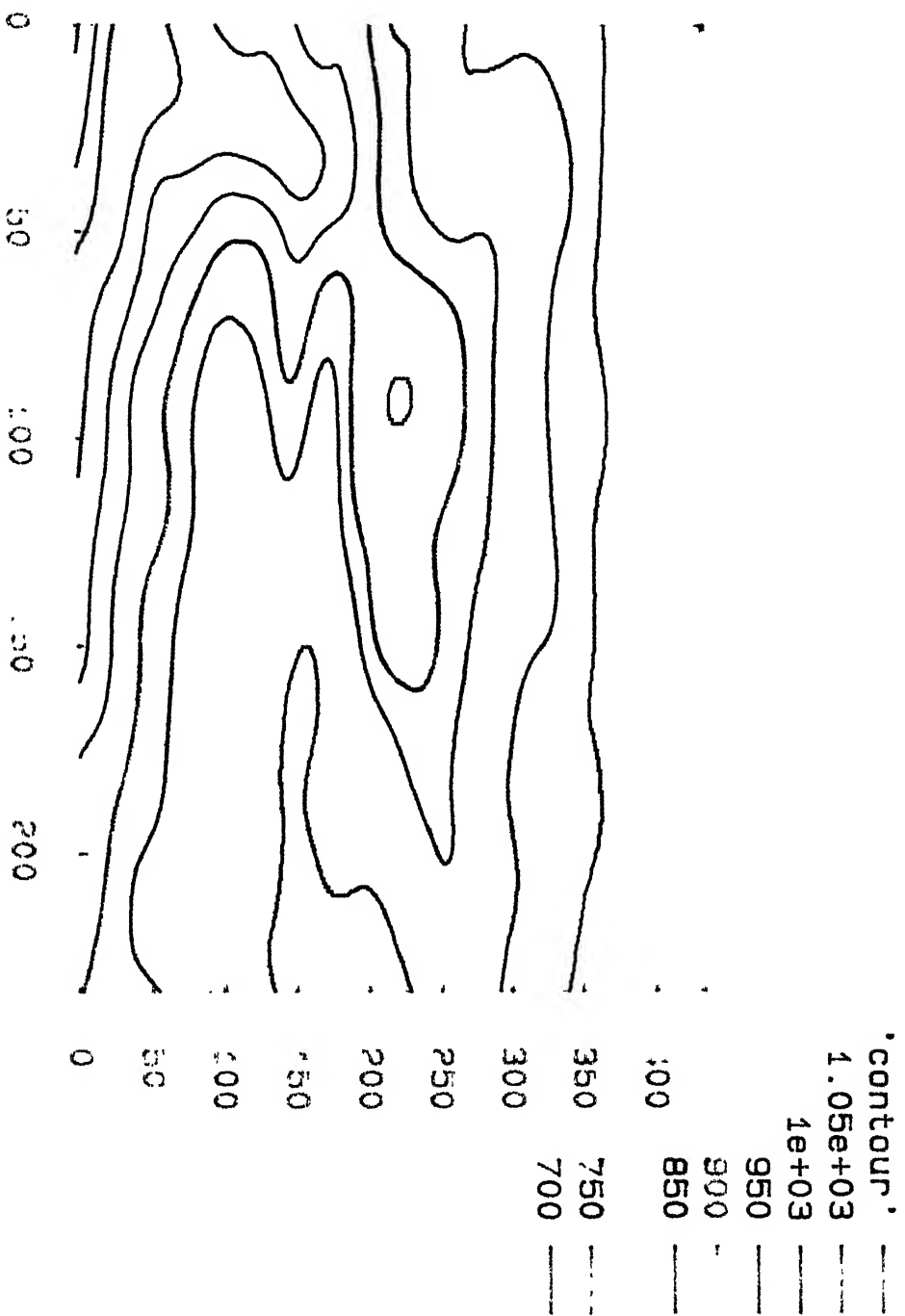


Figure 3.16.e

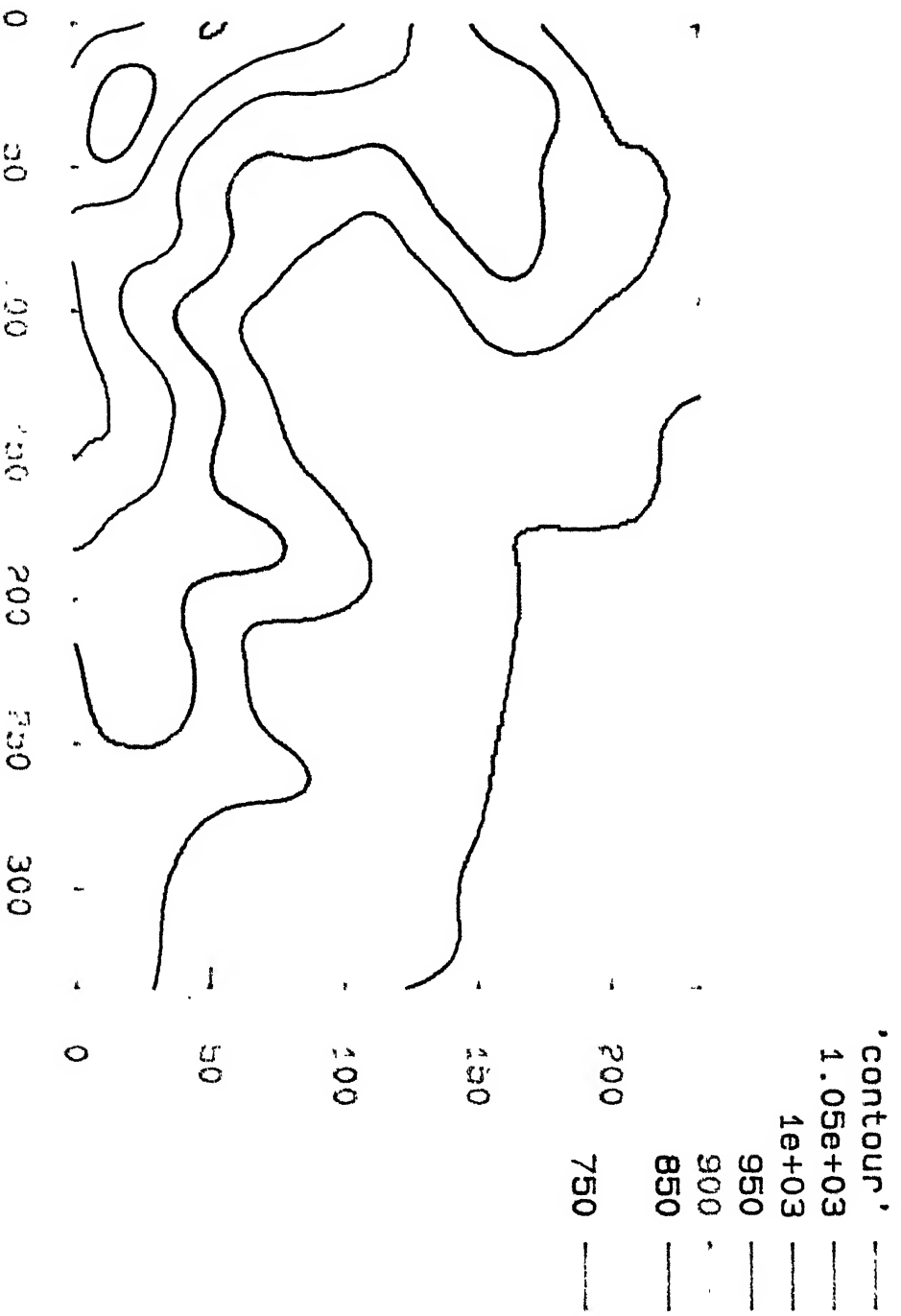


Figure 3.16.f

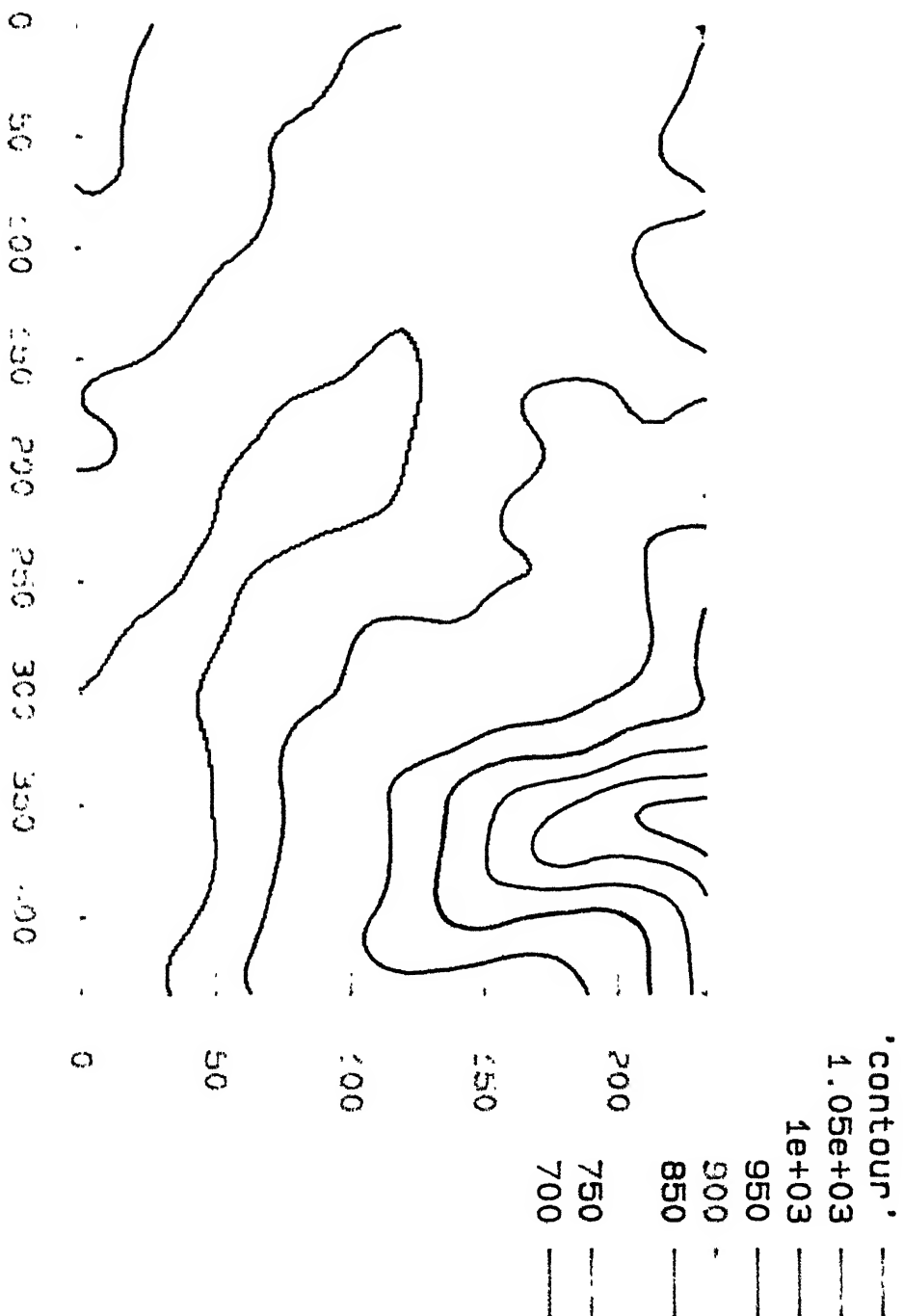


Figure 3.16.g

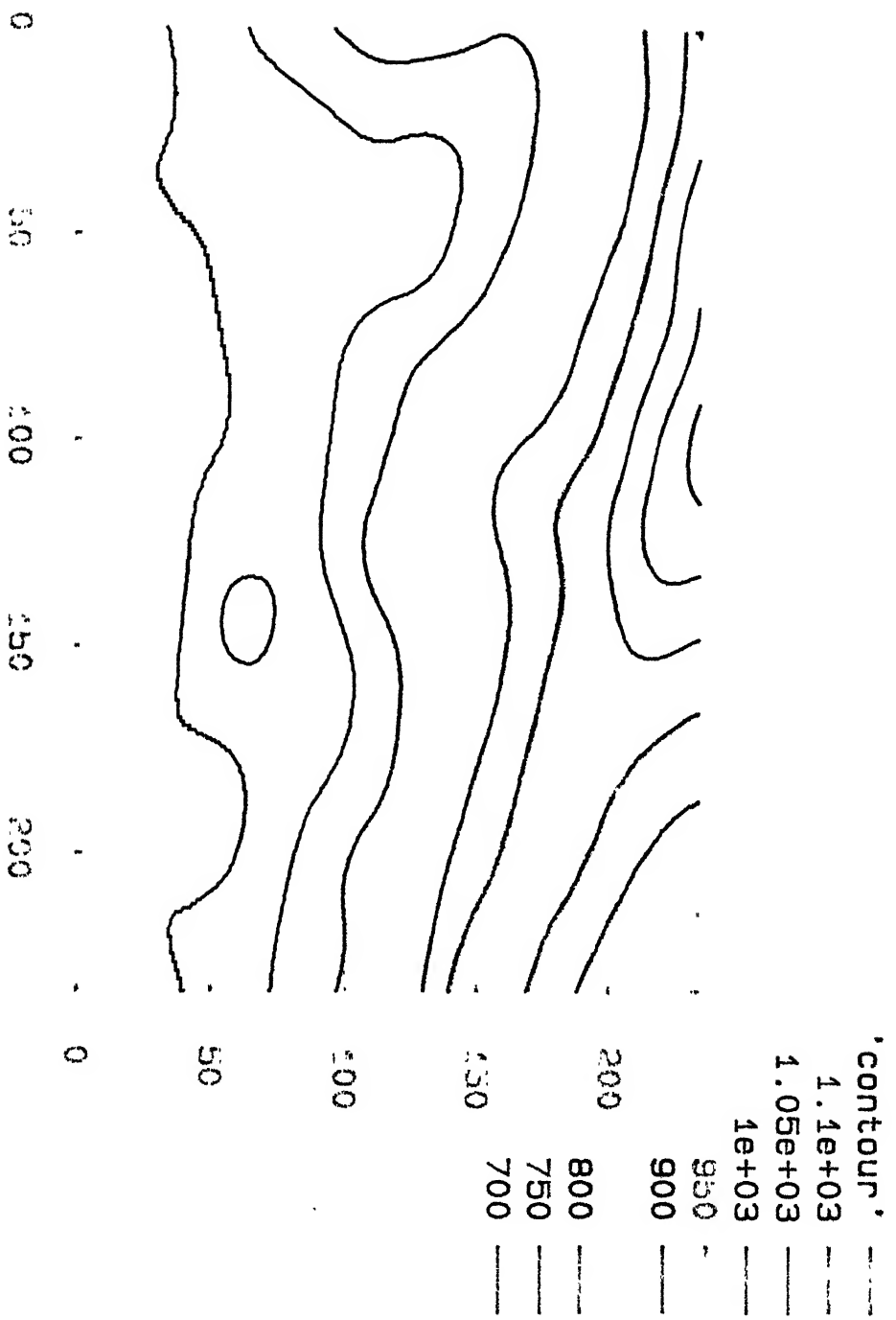


Figure 3.16.h

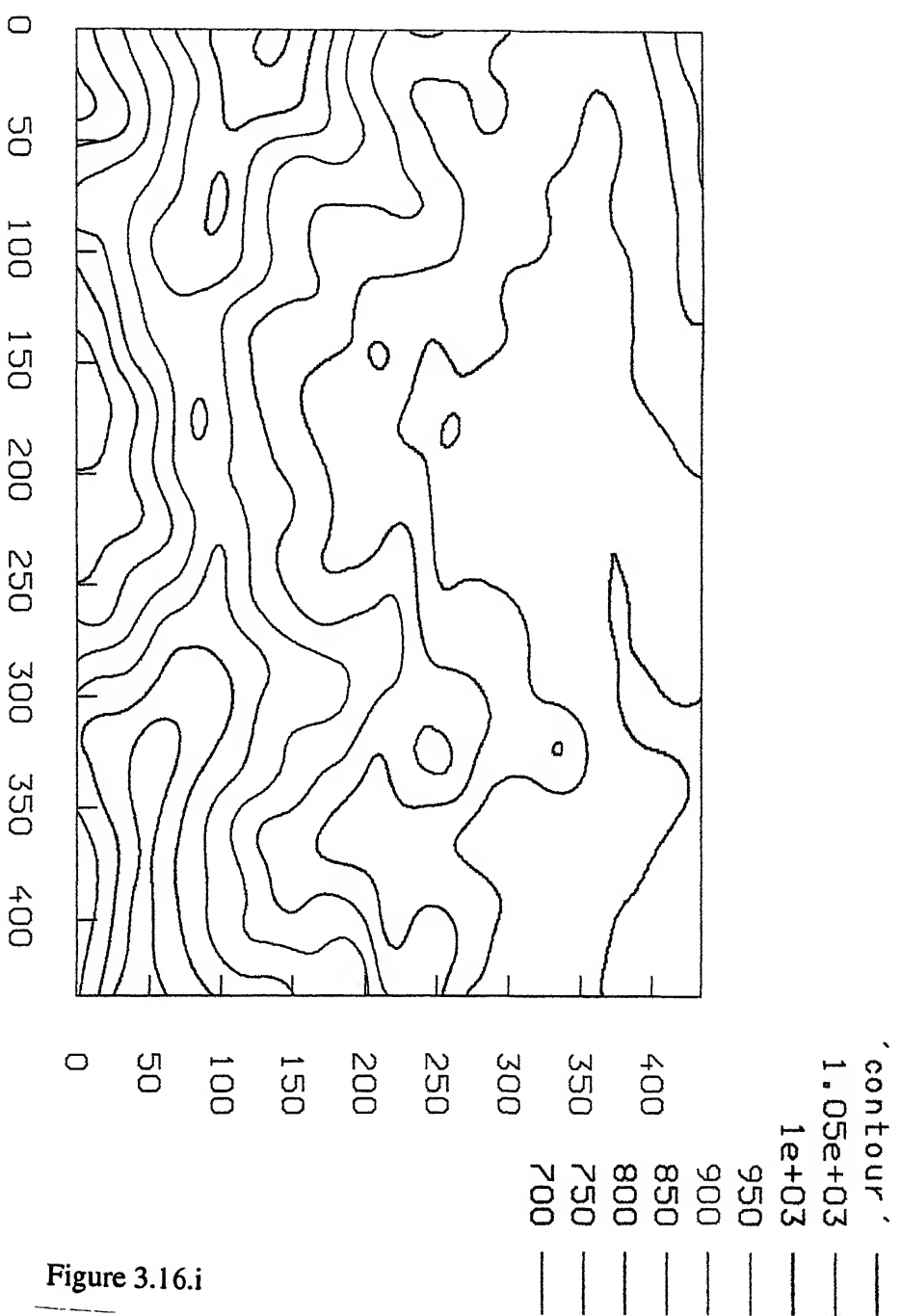


Figure 3.16.i

CHAPTER FOUR

CHROMO-STEREOSCOPY

4.1 Introduction

For a work to be conceivable it must be presented in a meaningful and realistic way. In general digital elevation data are presented in the form of height maps, height classified maps, slope maps. A new method of representing the terrain information is proposed as chromo-stereoscopy (Toutin and Rivard, 1995). In chromo-stereoscopy, the height data is coded into colours and the colours are decoded by means of special optics.

Chromo-stereoscopy is a concept for qualitatively perceiving depth. In this differently coloured objects at the same viewing distance appear to be at different depths (Einhoven, 1885). This apparent depth difference is further enhanced by a refraction process. These two phenomena can be used to perform fusion of multi-source remote sensing stereo data, and to qualitatively perceive depth from the single stereoscopic fused image. Chromo-stereoscopy examines depth perception from qualitative point of view, it does not extract quantitative depth information.

Depth perception and colour are two main criteria to visually sense the physical world. Depth perception is further found to rely on two different cues, namely primary and secondary. Primary cues are psychological and are associated with muscular accommodation activity in the binocular disparity of eye. Secondary cues are pictorial, which are used to explain depth perception in photos and images. These two cues jointly take into account the relative sizes of objects, hidden objects, shadow, linear perception, height of objects above the line of sight and difference in the focusing of the eye required for viewing objects at varying distances. Because eye and brain are part of the sensor system, some key aspects of their important role in this method are presented (Braunstein, 1976).

4.1.1 Eye: biological phenomenon

Human beings perceive objects by virtue of the light reflected or emitted by the objects with in the environment. This information is provided by eyes. Eyes play an important role in interpretation of the environment. The process of viewing does not merely consist of seeing but also involves perceiving and understanding through the central nervous system. The brain, eye starting with retina, involve in generating the picture of the objects. A prior knowledge about scene can be useful for better understanding and interpretation of the image (Hoffman, 1991). The eye and vision are very complex and sophisticated systems developed by nature. They involve physiological, biochemical, neurological and psychological processes. Eye has two kinds of receptors: cones and rods, these are having the shapes of cone and rod respectively. Cones are highly concentrated in the fovea and are in direct one to one connection with bipolar nerve cells. Rods are spread in the periphery of the retina and are connected with nerve cells. Rods and cones can have connection with the same bipolar nerve cell. Visual sharpness is less precise when using rods. Cones which are bigger than rods, are mainly used for detail study in bright light. Cones also give colour information. Rods, which are smaller but 18 times more numerous, are useful in reduced but are sensitive only to black and white light (Toutine, 1995).

4.1.2 Colour

Scientifically, colour theory begins with Sir Isaac Newton. In 1704, he described a number of experiments revealing puzzling properties of colours, using a prism he separated sunlight into spectrum of colours. Light of different wave lengths is refracted by varying degrees when passing from one medium to another. He distinguished seven colours whose wave length range from 4,000 to 7,600 Å.

A colour can involve variation in hue (chromaticity), intensity (brightness), or saturation (purity) separately, or it can involve more than one of these components. In certain region of spectrum even a variation of 5 to 10 Å, may be appreciated. Humans can discriminate 120 or more hues when intensity and saturation are constant. In reality, differentiation

begin to break down if more than seven to twelve along with black, white, and grey tones are used at the same time in a display (Mc Cormick, 1976).

At extremely low intensities, the retina shows a variable sensitivity with respect to wavelength, being most sensitive at about 5,000 Å in the green range. In day vision with cones, there is a characteristic shift to 5,600 Å. With low intensities red becomes much darker and blue much brighter. As darkness increases, the rod luminosity prevails over that of cones.

4.1.3 Visual Depth Perception

From the depth context, the visual system (the process) creates the three dimensional world from the two-dimensional pattern projected on the retinas. The fact that we can see the depth quite well with one eye closed, or in photograph or painting, may indicate that two eyes are not necessary for satisfying sense of depth. This dichotomy suggests an intimate relationship between object recognition and perception of three-dimensionality. In psychology, depth perception is based upon as many as ten cues (Braunstien, 1976). The cues are the additional pieces of information which, when added to a flat picture on the back of the eye, make depth perception possible. The brain combines these pictures with 2-D picture to produce the relationship of objects in space.

These ten cues are classified into two major groups: four physiological and six psychological for retinal image (Okoshi, 1976). The physiological cues are accommodation, convergence, binocular disparity, and motion parallax. Accommodation (focusing of distance) and convergence (moving the entire eyeballs) are associated with the muscular activity of the eyes, and are regarded as minor cues to depth, these are effective only at a distance of less than nine meters. The binocular disparity cue is related to the slightly different images of any given object which are received by the eyes. The degree of disparity between two retinal images, (binocular parallax) depends on the difference between the angles at which an object is fixed by the right eye and the left eye. For medium viewing distances, this cue is the most important for depth perception. For larger viewing distances the angular differences the two retinal images diminishes, which decreases the depth perception.

The six psychological cues which give depth sensation from planar images formed on the retina are retinal image size, linear perspective, overlapping, shade, shadow and texture gradient. These are combined together to enhance depth sensation. In remote sensing, perspective is found to be more useful cue and, in radar images, the shade and shadow cue for depth perception (Toutine, 1997).

4.2 Stereo Contemplation Approaches

In natural depth perception, stereoscopic pictures are viewed separately by each eye: the right image to the right eye and the left image to left eye. Many methods have been developed on basis of different concepts in recreating depth perception. Some of them are stereoscope, the anaglyph, and polarised glasses which allow left and right images to be seen respectively by the left and right eye. The 3-D shutter glasses are a more worldly device where shutter glasses are synchronised with a screen alternatively displaying left and right images. All above mentioned systems utilised the horizontal parallax to generate the depth perception.

The first attempt at a stereoscopic drawing was a technique by Giovanni Batista della Porta around the year 1600 (Okoshi, 1976). Recently in 1995, Sharp Laboratories in Europe claimed a major advantage in 3-D moving image technology (Toutin and Rivard, 1995). In producing the 3-D images using Liquid Crystal Displays (LCDs), the twin LCDs are placed at right angle to each other. The images are then combined by a exclusive optical filter that transmits the image from one display, and reflects the image from the other, producing a 3-D image.

Most of these stereoscopic images have a common feature: the representation of a separate view to each eye with horizontal binocular parallax. All the 3-D imaging techniques described above relied upon two cues: binocular parallax and convergence. The invention of holography (Gabor, 1948) is particularly significant because it offered for the first time a method of spatial imaging with the accommodation cue. Holography consists of two step lens less imaging process, the hologram is first recorded as an interference pattern, generated by the interaction of scattered monochromatic light from an object and

a coherence reference wave. The second step involves the reconstruction of the optical field or image through the diffraction of a coherent beam by the transparency, which is the developed hologram. In holography the interference pattern contains, by way of the fringe configuration, information corresponding to both the amplitude and the phase of the wave scattered by the object.

4.3 Chromo-Stereoscopy

Einhoven proposed the Chromo-Stereoscopy concept as early as 1885. In this phenomena, the colour objects present on the same plane appear at different depths. In positive chromo-stereopsis the objects with red colour have higher apparent elevation in comparison to objects with blue colour, while opposite sense of colour objects is called negative chromo-stereopsis. Einthoven proposed that this phenomena is due to the chromatic dispersion and relation between the visual and optical axes. It is possible to enhance the chromo-stereopsis by controlling the refractive properties of the material used in making lenses. The amount by which the light refracts when it passes from one medium to another is completely dependent on the speed of the light in those mediums. The speed of the light is depend on the wave length of light. The division of a white light into different colours when it passes through a prism is a good example of this concept.

The basic concept in generation of the chromo-stereoscopic image is to classify the depth present in the image by means of assigning colours, and decoding the coloured image by means of special optical instrument. In the process of generation of these optical instruments glasses made with prisms (plastic, glass, fresnel) worked extremely well, but the production of such instruments on large scale is found to be uneconomical. Later research community experimented with thin diffractive optics. These lenses incorporate a high precision system of micro optics. When light passes from one medium to another it produces differential angular parallax by virtue of its dependence on the refractive index value of the material and wave length of light. An example of this is shown in Figure 4.1. When light passes through single prism glass, it is subjected to deviation, this deviation of

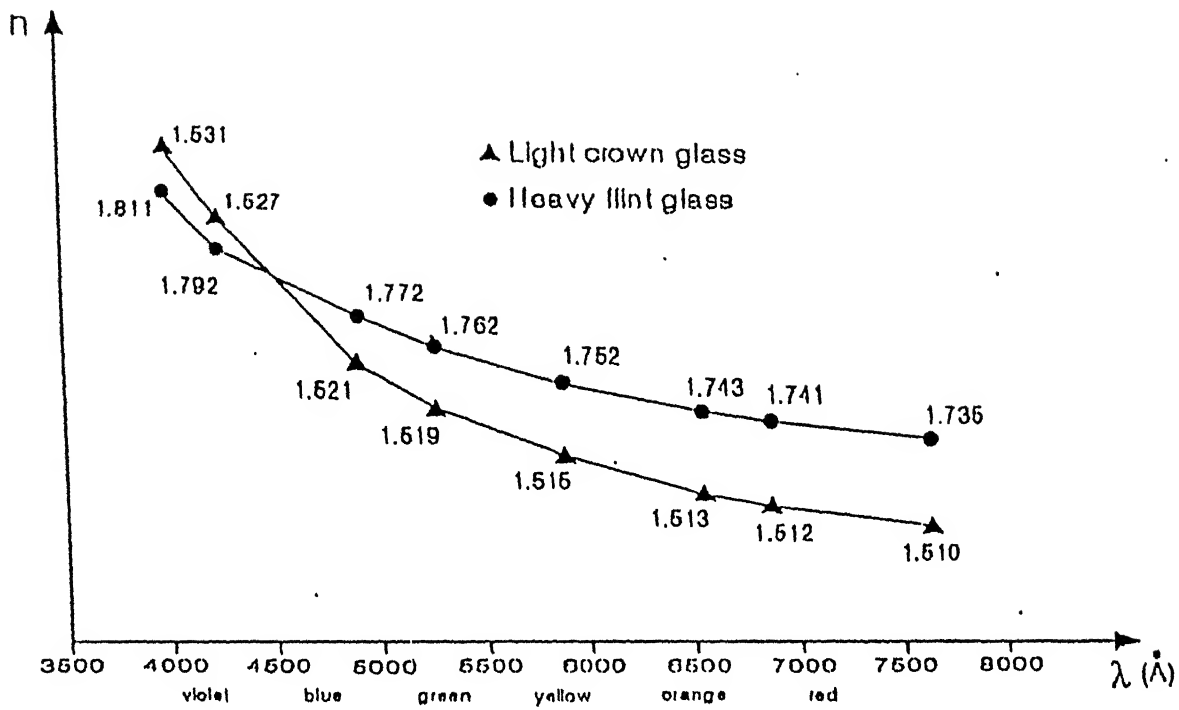


Figure 4.1 Variation of refractive index with respect to material and wavelength
(source: Toutine, 1997)

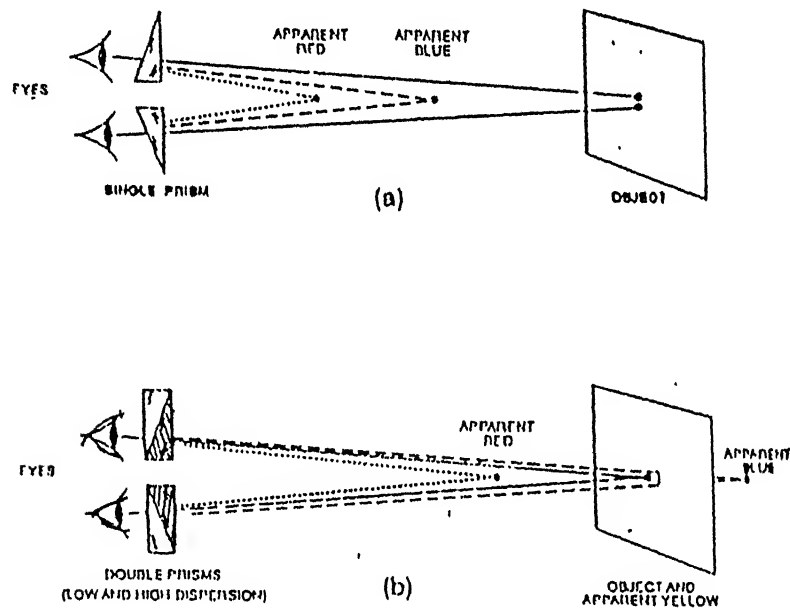


Figure 4.2 (a) Single prism glass configuration, (b) Double prism glass Configuration
(source: Toutine, 1997)

light makes the object appear much closer to the eyes (shown in Figure 4.2.a). This gave rise to two major problems (Steenblik, 1986,1991):

1. because of this deviation of light rays, the object appears to be shifted from the focal point of the eyes, this causes strain to the eyes.
2. while looking at the object if the user changes his position, the object moves differently from what the brain anticipates. This results in visual disorientation of the sight.

To rectify both the above mentioned problems, double prism glasses are used. This pushes the object back to the position at which it was supposed to appear (shown in Figure 4.2.b). The two prisms used, a low dispersion and a high dispersion are designed in such a way that the deviation of yellow light is zero, and the other colours deviate with respect to their wave lengths. Because of the high dispersion prisms, red objects appear at higher level than the objects having blue colour.

4.4 Methodology

In remote sensing projects, after the acquisition and communication stages, lies a very important stage of data processing and visualisation. The level of automatic processing of the data to obtain information, depends on the specialised tools and systems used by the human interpreter in analysing the study area. Colour and stereo are two main characteristics of eyes. Colour conveys information about multi-dimensional data (Ware and Beatty, 1988), and the use of colour can significantly aid users in perceiving information and making inferences (Eastman, 1971). Depth perception can be facilitated by using 3-D, which can improve the interpretation of cartographic data. This shows an interest in stereo and colour pictures and how our eyes and brain visualise with machine handled displays and symbols. Chromo-stereoscopy is an interesting tool to help human interpreters understand terrain representation in the remote sensing images and to perceive and extract very useful information. In order to generate a quality stereoscopic image six important steps have to be carried.

The first step in this process is geometric correction. Precise geometric correction is very essential, because the clarity of the chromo-stereoscopic image is very sensitive to the registration of the image, and any error in registration will induce blur in chromo-stereoscopic image. This is followed by extraction of the height information from the

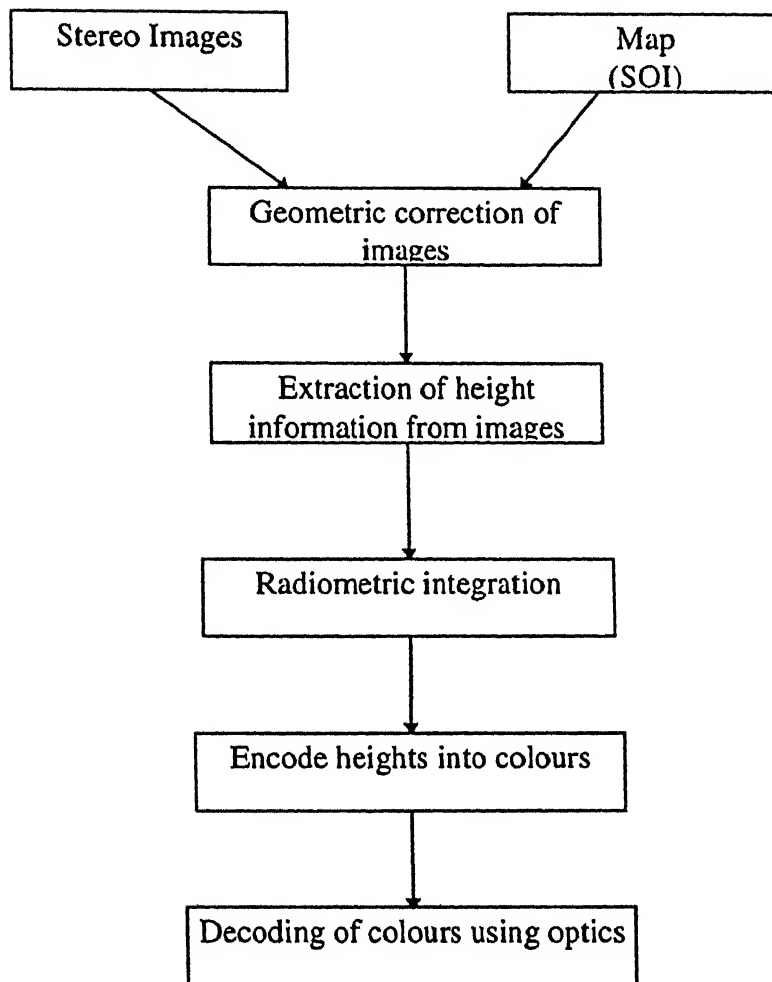


Figure 4.3 Flow Chart for Generating Chromo-Stereoscopic Image

stereo images. Digital photogrammetric methods are used in generating relative and absolute digital terrain model. Once the height information is obtained, it is coded into colours. The range of heights to which colour to be assigned is very important. Pixels with relatively high relief are assigned red colour, the one of lower range are assigned blue colour and finally the terrain having relief in-between this range is assigned green colour.

Another very important step in this process is the radiometric integration. In this the characteristics of the surface is imparted to the chromo-stereoscopic image by giving the intensity of colour, the grey level value of the remotely sensed image. Finally the chromo-stereoscopic image is decoded by using ChromaDepth glasses (thin double prism glasses). Flow chart of this process is given in Figure 4.3.

In the present work, geometric correction of the data is performed by non-parametric approach (polynomial transformation method), which is explained in Chapter Three. The software developed generates the height information which is provided as the input height data file to this module. It is found that terrain vary from 600m to 1150m, with major chunk of the area ranging between 650m to 1000m in the study area. Terrain with relief less than 780m is assigned blue colour, green colour is assigned to area with relief range of 780m to 900m, and terrain with relief more than 950m is assigned red colour. This module is designed in such a way that range of look up tables can be changed. The image intensities were found to range between 22 to 103. Four different chromo-stereoscopic images were developed with their maximum intensity limited to 127, 115, 105, 95 . It is found that as the maximum intensity value reduce the sharpness of the image is increased. The chromo-stereoscopic image with its intensity maximum value compressed to 95 is shown in Figure 4.4.

4.5 Analysis of Chromo-Stereoscopes

The chromo-stereoscope of the study area has been generated using the methodology discussed earlier and the same is shown in Figure 4.3. When viewed with ChromaDepth™ glasses the whole terrain appears in three dimension. The elevation appears in descending from red, green, blue and black. In the central portion from right top corner to lower left

corner, a ridge line appears in red shades. In upper left portion lies Tanaji sagar, a very large lake in black colour with numerous tributaries branching from ridge lines. Valley

portion is shaded with blue. In right bottom corner geomorphic details of Kanand Nadi is shown with black colour in blue zone. Whitish zone depict populated zones, roads etc.,. They appear above the ground in blue and green area of the image. Roads and built-up regions are characterised with high intensity of reflectance. Here, they being coded in intensity channel and having very high blue and green reflectance appear almost white. This image produces Crystal clear contrast between high and low profiles and viewers perceive the whole terrain in virtual reality.

4.6 Conclusion

Present work is an attempt to present the concept of Einthoven, floated in 1885 i.e., chromostereoscopy for the case of global relief viewing of terrain generated using digital photogrammetry. This has produced a synthetic 3D of regional picture by presenting ridges, valleys, lakes, rivers in their natural relief. This serves as an effective mode of reconnaissance for project planners and administrators. This may find tremendous application for geological exploration, civil engineering project siting and of course war planning strategies.

SOFTWARE DEVELOPMENT

The aim of this work is to develop software package for generating height information from stereo images and to represent the height information in various eloquent ways. The complete *Softcopy Photogrammetric and Chromo-Stereoscopic System* is illustrated in the Figure 5.1.

5.1 Hardware and Compilers

The software development has been performed on following hardware and compilers.

- HP TRSX 98731 Work Station series.
- DEC ALPHA

Following inbuilt compilers and graphics library are used

- UNIX operating system is used.
- C and ANSI C Compilers are used.
- STARBASE graphics supported on HP workstation.

5.2 Geometric Correction

Software developed for various operations of geometric correction, are as follows:

5.2.1 GCP generation

The ground co-ordinate positions are determined by using ILWIS Digital Image Processing System. The suitability of a GCP for geometric rectification is determined by what proportion of the total planimetric error it is contributing. This analysis is carried using `coeff.c` program.

5.2.2 Registration

Code is generated for the registration of the images on to the common co-ordinate system (`regis.c`). The GCPs selected are used in calculating the

coefficients of transformation equations(mult.c, mult1.c, mult2.c). The radiometric resampling is performed using nearest neighbourhood method in regis.c.

5.3 Cross-Correlation and Height Determination

The parallax at a point is determined using para.c. In this the input is registered left and right image. This program generates the relative heights using cross-correlation function. The output from this program is a parallax file.

5.4 Input File for Display of DTM

The code expects the height file data in integer form. In this total height file as well as a part of the height file can be used. The extraction of height information for small areas is carried using the initially calculated transformation co-ordinates.

5.5 Core System

The complete overview of the system comprising of developed software and hardware is illustrated in Figure 5.1. Each sub module is discussed in brief.

5.5.1 Display of Image

This module is used to generate the image from the digital data file. This responds by asking for the file name, and then the number of rows and columns. This module is also provided with the linear contrast enhancement, which is used to display the contrast stretched image. After the user providing the information about the input image file, program asks for the display co-ordinates of the top left corner of the image, then it displays the image on to the screen. The images displayed by this module are shown in Figure 1.2 and 1.3.

5.5.2 Display of Height Map

This module is used to generate the grey intensity height map. This module requires the input of height data file, with data in integer form and the rows and columns of the

height map. After the input is given to the system, it calculates the maximum and minimum height values. It then divides the intensity range into the levels which is equal to the maximum height of the terrain, i.e., it assigns maximum intensity value to maximum relief value and the other height data are assigned the intensity, which is proportional to its relief value. The height map of the present terrain is shown in the Figure 3.11.

5.5.3 Height Classified Map

This module works in the same way as explained in the display of height map, but with the difference that the image is classified on the basis of the relief. The intensity levels are restricted to the number of classes into which the image is classified. The extra input required in this module is the number of classes and their range of the heights. Then the complete height map is divided into different classes. The output of this module for the test data is shown in Figure 3.12. The range of heights of the class and the intensity are displayed along with the height map.

5.5.4 Mesh Model of Relief Data

Height data can be represented in many forms, out which 2D representation is shown in Figure 3.11 and 3.12. In this module the height information is represent in the form of a transparent surface. This gives an impression of floating mat in air. This module requires height data along with the number of rows and number of columns. This program can be used to develop the mesh surface by considering the input all pixel positions or at some user defined regular intervals. Both the methods are tried, and it is found that surface model is more appealing when the data at regular intervals is used. The test area mesh surface is shown in Figure 3.13.

5.5.5 Solid Model of Surface

This model is similar to the mesh model of surface generation with a difference that the surface is represented in solid form to give more realistic appearance to the terrain. This also requires the height data and number of rows and columns as input. Surface

is generated by representing the relief as 3D polygon at each pixel. This module consumes more time in comparison to the mesh model. Solid surface generated for the test area is shown in Figure 3.14.

5.5.6 Chromo-Stereoscopic Module

This module is used to generate the chromo-stereoscopic image of the test area. The technique used in developing the chromo imagery is explained in detail in Chapter four. This module requires height data file, number of rows, and number columns to read the file into the system. The input is processed, system asks for the height ranges for the red, green, and blue colours. To represent the terrain characteristics the intensity values of these colours are given, the original intensities of the stereo image, it then creates the chromo-stereoscopic image of the site area. Chromo-stereoscopic image of the test area is shown in Figure 4.4.

5.5.7 Slope Map

Slope map requires the height information of that area. This module require height map information as its input. Height data along with number of rows and columns is provided as input. This module calculates slope of a pixel by comparing its height with the eight neighbouring pixel relief information. This then prints the slope data file. Using the same slope data file it classifies the entire area into different classes. Generally six to eight classes are used in classification. The slope classified map is shown in Figure 3.15, in which the slope is classified into six different classes.

5.5.8 Contours

In the present software system no special code is written for contour. This module makes use of the GNU plot, which is a very good graphic package for generating contours. This module generates contour maps by linking the height data to the GNU plot by executing a shell file, code is written for executing this file with in the program itself without coming out from the program. Contour maps for the entire test region

are shown in nine plots, as the GNU software cannot work with very large data sizes. Grid size, with maximum of 350×350 can be given as input. The contour plot along with surface is shown in Figure 3.16 (a,b,c,d,e,f,g,h,i).

5.5.9 Output

This module is used to print the images into bitmaps. To obtain the output images into bitmaps, first the image has to be displayed on the screen, then this module is invoked to print the image into bitmap.

5.5.10 List

This module is used to display the list of images and list of bitmaps in the database.

5.5.11 Exit

Each module described above is provided with a option for exit, at the end of display of the image. This module is used for exiting from the software, without executing any of the display module.

The complete assembled software is provided in **soft3d.c**. The code of which is available with the author and the thesis supervisor. The executable is in the name of the code program name.

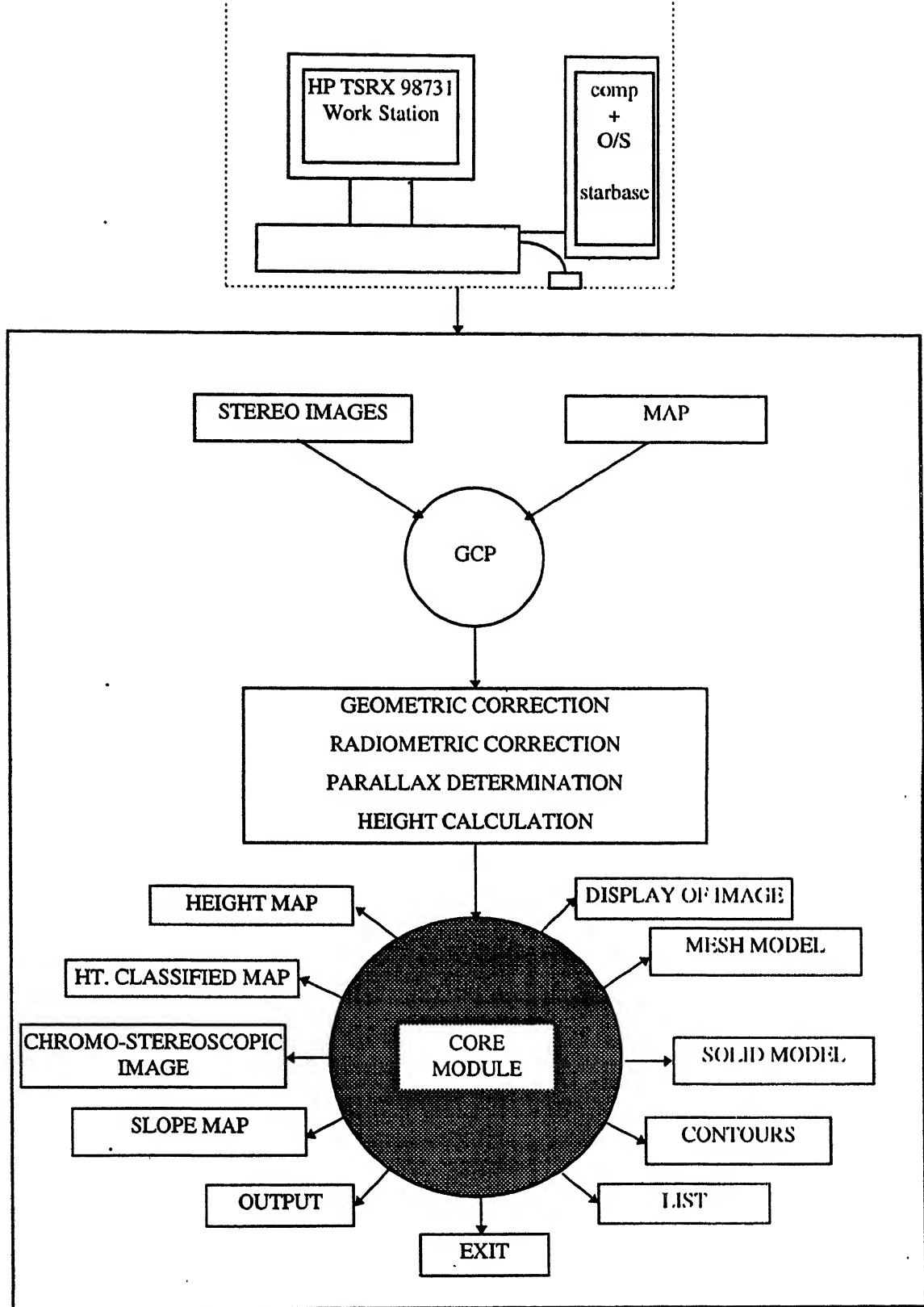


Figure 5.1 Softcopy Photogrammetric and Chromo-Stereoscopic System

CONCLUSIONS AND FUTURE RECOMMENDATIONS

6.1 Conclusions

The present work is dedicated for investigating an alternative to analogue photogrammetry, and also as an alternative to costly software and hardware required for digital photogrammetry. Since 1986 there has been a resurgence of activities related to satellite stereo data. Several researchers have done the work related to development of digital terrain model, from their experience and present work, area based matching has been found to be most appropriate technique for stereo correlation.

Earlier people used to work with parametric method of establishment of epipolar geometry, but the latter research has showed that non-parametric method which is simple and less time consuming has good accuracy. A complete software package has been developed by author which have modules like height map display, height classified map, mesh and solid surface modelling, slope classified maps, contours. The output from these modules can act as a data base and directly incorporated with GIS for any kind of studies in civil engineering projects.

A relatively new concept of softcopy photogrammetry in remote sensing has been applied which is based on depth perception by coding the relief in set of colours. The height data recorded from that been used for creating chromo-stereoscopic image (shown in Figure 4.4). It is envisaged that administrators and planners will find this technique very handy for analysing any terrain for development or mitigation of hazard. Even this phenomena can be adopted for generating complete atlas of country and can be used to educate children.

The softcopy photogrammetry package generated is user friendly and interactive. In this the software prints the data items required for the generation of the necessary output,

using which even laity can work on this system. Contour maps has been generated for the complete terrain. Survey of India provide the revision of information at large time gaps, using this software package we can get a real time topographic and contour data. This contour maps can serve for different kind of analysis and application such as route planning, irrigation and water distribution network, management of existing water bodies, profiling and cross sectioning.

Following conclusions based on present work are made :

1. The use of non-parametric method in establishment of epipolar geometry has given satisfactory results in height values.
2. From target window size analysis, target window size of 7×7 is suggested as the best window size.
3. The RMS error from the analysis at few selected points is 17.42m, which is good accuracy for reconnaissance works.
4. A complete Softcopy Photogrammetry System is generated.

6.2 Future Recommendations

1. Since the area is developing, it was difficult to locate ground control points, which has affected the planimetric accuracy of the registered images, which had an adverse affect on the accuracy of the height data determined. It is suggested that for such studies at least four artificial ground control points should be erected before ordering the satellite data. On these points accurate GPS co-ordinates can be established which should be used for geometrically rectifying the image for establishing epipolar geometry.
2. The spatial resolution of SPOT-PLA data is 10m, now data with 5.8m spatial resolution is supplied by IRS-1C PAN camera. This may be used for better accuracy as ground control point locations can be located much precisely.
3. Though the software has been made user friendly, yet there is a scope for more modules and documentation.

4. The study has opened access to tremendous data base which may be readily used in GIS for integration of stereo photogrammetry and GIS may be an interesting future research area.

REFERENCES

- Brockelbank, D. C., and A. P. Tom, 1991. Stereo Elevation Determination Techniques for SPOT Imagery, *Photogrammetry Engineering & Remote Sensing*, 57(8):1065-1073.
- Braunstien, R. L., 1976. *Depth Perception through Motion*, Academic Press Inc., New York, USA.
- Berthold, K. P. H., 1983. Non-Correlation Methods for Stereo Matching, *Photogrammetry Engineering & Remote Sensing*, 49(4):535-536.
- Cappellini, L., I. Alparene, G. Galli, P. Lange, A. Mococchi, and L. Menichetti, 1991. Digital processing of Stereo Images and 3D Reconstruction Techniques, *International Journal of Remote Sensing*, 12(3):477-490.
- Chevreil, M., M. Courties, and G. Weill, 1981. The SPOT Satellite Remote Sensing Mission, *Photogrammetry Engineering & Remote Sensing*, 47(8):1163-1171.
- Ehlers, M., and R. Welch, 1987. Stereocorrelation of Landsat TM Images, *Photogrammetry Engineering & Remote Sensing*, 53(9):1231-1237.
- Einthoven, W., 1885. Stereoskopie durch Farbendifferenz, *Albrecht von Graefes Archiv fur Ophtamologie*, 31:211-238.
- Gabor, D., 1948. A New Microscopic Principle, *Nature*, (161):777-779.
- Gruen, A. W., 1989. Digital Photogrammetric Processing Systems Current Status and Prospects, *Photogrammetric Engineering & Remote Sensing*, 55 (5): 581-586.
- Hoffman, R. R., 1990. Remote Perceiving: A Step Towards a Unified Science of Remote Sensing, *Geocarto International*, 5(2):3-13.

Kennie, T. J. M., and G. Petrie, 1990. *Engineering Surveying Technology*, Blackie, Glasgow and London.

Malleswara Rao, T. Ch., K. Venugopal Rao, A. Ravi Kumar, D. P. Rao, and B. L. Deekshatulu, 1996. Digital Terrain Model (DTM) from Indian Remote Sensing Satellite Data from the Overlap Area of Two Adjacent Paths using Digital Photogrammetric Techniques, *Photogrammetry Engineering & Remote Sensing*, 62(6):727-731.

Mather, P. M., 1987. *Computer processing of remotely Sensed Image: An Introduction*, John Wiley & Sons, Newyork.

Richards, John. A., 1993. *Remote Sensing Digital Image Analysis: An Introduction*, Springer - Verlag, Berlin.

Rosenberg, P., 1955. Information Theory and Electronic Photogrammetry, *Photogrammetric Engineering*, 21(4):543-555.

McCormick, E. S., 1988. Art, Illusion and the Visual System, *Scientific American*, 258(1):78-85.

Okashi, Th., 1976. Three Dimensional imaging techniques, *Academic Press Inc.*, New York, USA.

Steenblik, R. A., 1986, 1991. Stereoscopic Process and Apparatus Using Different Deviations of Different Colours, *U.S Patents* No. 4-597-634 and 9-002-364.

Theodossiou, E. I., and I. J. Dowman, 1990. Heighting Accuracy of SPOT *Photogrammetry Engineering & Remote Sensing*, 56(12):1643-1649.

Welch, R, 1980. Measurements from Linear Array Camera Images, *Photogrammetry Engineering & Remote Sensing*, 46(3):315-318.

Ware, C., and J. C. Beatty, 1988. Using Colour Dimensions to Display Data Dimensions, *Human Factors*, 30:127-142.

Welch, R., 1983. Impact of geometry on Height Measurements from MLA Digital Image Data, *Photogrammetry Engineering & Remote Sensing*, 49(10):1437-1441.

Toutine, Th., and B. Rivard, 1995. A New Tool for Depth Perception of Multi-Source Data, *Photogrammetric Engineering & Remote Sensing*, pp 1029-1031.

Toutine, Th., 1997. Qualitative Aspects of Chromo-Stereoscopy for Depth Perception, *Photogrammetric Engineering & Remote Sensing*, 63(2):193-203.

Wolf, P. R., 1995. *Elements of Photogrammetry*, Mc Graw-Hill Book Company, New Delhi.
